ACOUSTICAL PROPERTIES IN SUPERCONDUCTING NIOBIUM

By

GARY WAYNE GOODRICH

Bachelor of Science
University of Texas
Austin, Texas
1966

Bachelor of Arts
University of Texas
Austin, Texas
1966

Submitted to the Faculty of the Graduate College
of the Oklahoma State University
in partial fulfillment of the requirements
for the Degree of
MASTER OF SCIENCE
May, 1968

ACOUSTICAL PROPERTIES IN

SUPERCONDUCTING

NIOBIUM

Thesis Approved:

James Lange
Thesis Adviser

H E Harrington

N Durham
Dean of the Graduate College

ACKNOWLEDGMENTS

The author is grateful to the National Science Foundation for financial support during part of this investigation. The guidance, assistance, and discussion time of Professor James Lange, Jr., is appreciated. Also, Professors George Thurston, Herbert Pohl, Thomas Winter, and William Leivo contributed by lending equipment necessary to conduct this investigation. Gordon Nelson, Jr., helped take these measurements and will be continuing the study of niobium through magnetization measurements. The Physical Science Machine Shop and Glass Shop helped build much of the experimental set-up. The help with calculations and typing assistant of my wife, Patti, is appreciated.

TABLE OF CONTENTS

LIST OF TABLES

LIST OF FIGURES

CHAPTER 1

INTRODUCTION

Low frequency acoustical measurements of Young's modulus and the associated attenuation coefficient as a function of magnetic field have been performed on single crystal and poly crystalline niobium (Nb) in the superconducting region. The purpose of this investigation is to detect changes in these physical properties of the Nb crystal which may give a better insight into type II superconductivity. The experiment utilizes a parallel plate capacitor transducer technique with the sample serving as one plate of the capacitor. This method may be used for comparison with data taken by other means. The shear modulus may also be measured with this same apparatus. Moduli changes may be measured to one part in 10^9. Typically a Q of 10^6 is measured in Nb. The attenuation is measured by the free decay method (1) within an experimental error of less than 5%. The time rate of change of the voltage amplitude from the resonant frequency signal of the cylindrical Nb rod was used to measure the attenuation coefficient, or loss factor. The velocity of sound in the material may also be computed from this data. Magnetization measurements have been made in conjunction with this work in order to determine when the sample began to change phase into the mixed state, H_{C1}.

CHAPTER II

THEORY

Superconductivity has several general features. The word "superconductor" arose from a state of matter with zero electrical resistivity, i.e., it is a "super" conductor. A superconductor is better characterized by its diamagnetic suseptibility. The perfect diamagnetism resulting in the Meissner effect (2) is the fundamental basis of superconductivity. At the transition temperature between superconducting and normal states other physical parameters also experience unusual changes, e.g., the heat capacity is discontinuous (3).

Superconductivity

Superconductors can be classified by two types (3). Type I is distinguishable by an abrupt change in resistivity, and other parameters, at the interphase between superconducting and normal states. Type II is distinguished by a gradual change of magnetization, or other parameters, from one state to the other through what is termed the intermediate, or mixed state. Nb is a type II material, as are most alloys. Most pure metals are type I. The penetration depth, λ, gives the depth that an external magnetic field can penetrate into the superconducting sample (4). Another term, the coherence length ξ, is the distance between strongly interacting electrons and is usually the order of 10^{-4} cm (4). The superconducting state is a lower energy state than the normal state

by an energy gap of Δ. Electron pairs, called Cooper pairs (5), form and drop the system to the lower energy of the superconducting ground state. The relation of the coherence length to the penetration depth determines the type of superconductor. For $\xi > \lambda$, type I superconductors are formed, and $\xi < \lambda$ indicates a type II superconductor.

Type I superconducting properties have been formulated into a microscopic, or quantum mechanical, theory called the B.C.S. theory (5). This theory has accounted for all of the experimentally observed phenomena up to date. It accounts for the electron pairing, the energy ground state of a superconductor, the penetration depth, the coherence length, the Meissner effect, and the transition temperature. It is the electron pairing that reduces the resistivity to zero in the superconducting state. Attenuation of acoustical waves is due partly to the conduction electron scattering from the phonon (or lattice) field while in the normal state. When the material undergoes a superconducting transition, the attenuation is reduced as the electron pairs themselves lower their energy.

The B.C.S. theory fails to predict type II superconductivity. While the mechanism of both types is the same, i.e., electron-phonon interaction (3), the magnetic properties of the superconducting-normal transition are entirely different between the two types. This type II superconducting transition may be caused in several ways. It is necessary to supply the electron pairs with enough energy to jump the gap into the normal state. The temperature may be raised above the critical temperature to restore the normal state. Critical temperatures for all materials known today are below 20° K. Raising the temperature amounts to supplying thermal energy. It is also possible to optically excite

electron pairs across the gap into the normal state (6). Alternately, a magnetic field of sufficient intensity will destroy the superconducting state and restore the normal state by decreasing the energy gap. Lower temperatures require higher magnetic fields for this transition.

The Meissner effect is observed in a material immersed in a uniform magnetic field when it is cooled below the transition temperature. In the superconducting state the lines of flux B are ejected out of the sspecimen (2). When a type I specimen in the superconducting state is exposed to a uniform critical field, H_c, the magnetic field suddenly penetrates the specimen fully, and the normal state is regained. In type II materials at a lower critical field, H_{C1}, the magnetic field lines begin to penetrate the sample. Then at a higher field, H_{C2}, the field finally penetrates the material completely and the normal resistivity returns. The mixed state exists between H_{C1} and H_{C2} where the normal and superconducting states are believed to coexist. As the field begins to penetrate a type II material, it enters the sample in quanta with flux jumps observed in some materials (7). To satisfy Maxwell's electrodynamic equations, the magnetic field B must have only a tangential component at the surface of the material. A normal component would imply a discontinuity in the magnetic field and contradict div B = 0. The surface currents of the superconductor shield the inner material from the magnetic field, leading to the Meissner effect.

Thermodynamics can be used to describe the phase transition from the superconducting to normal state by means of the magnetic energy term (4). When the first law of thermodynamics is extended to include the magnetic term, it becomes

$$dU = TdS - PdV + HdM$$

where H is the magnetic field and M is the magnetization per unit volume. For a perfectly diamagnetic superconducting state

$$M = -H/4\pi .$$

Therefore,

$$dU = TdS - PdV - HdH/4\pi .$$

Using the Gibbs potential,

$$dG = VdP - SdT + HdH/4\pi .$$

Thus, at constant temperature and pressure,

$$\Delta G = H_c^2/8\pi$$

where H_c is the critical field. H_c for a type II superconductor is defined so that $H_c^2/8\pi$ equals the difference of thermodynamical potential density between the normal and superconducting states in zero magnetic field (3). The free energy difference between the superconducting and normal phase is

$$\Delta F = H_c^2/8\pi = \Delta U - T\Delta S .$$

Nernst's Law states that at absolute zero of temperature, ΔS must be zero. Therefore, the energy gap is given by

$$\Delta U = H_c^2(0)/8\pi$$

where $H_c(0)$ is the critical field at absolute zero in temperature. From the B.C.S. theory (5) for type I superconductors, this energy gap is calculated to be $3.52kT_c$, where k is Boltzmann's constant and T_c is the critical temperature. The latent heat of transition from the superconducting to normal phase is given by

$$L = -(T H_c/4\pi) \frac{dH_c}{dT} .$$

This latent heat of transition implies a first order phase transition for type I superconductors. A second order phase transition would mean a discontinuity in dS/dT, rather than a discontinuity in S, as is the case for a latent heat. As the temperature approaches the critical temperature, the magnetic latent heat approaches zero. For a transition in zero magnetic field, a first order phase transition occurs. Another

term involving the stress and strain may be added to the differential Gibbs's function equation:

$$dG = -SdT + VdP - MdH - \sum \tau_i d\sigma_i$$

where τ_i is the strain per unit volume and σ_i is the stress (8). Phase transitions are related to the discontinuities that appear in the derivatives of the Gibb's function. A discontinuity in the Nth derivative implies an Nth order phase change.

$$\frac{\partial G}{\partial \sigma_i} = -\tau_i \quad .$$

Thus, a discontinuity in the strain would mean a first order phase transition. Since the strain in related to the stress by

$$\tau_i = \sum S_{ij} \sigma_j$$

where S_{ij} is a stiffness constant.

Therefore,

$$\frac{d\tau_i}{d\sigma_j} = S_{ij} \propto m^{-1}$$

where m is the effective elastic constant, or modulus. Then a second order phase transition would result by a discontinuity in

$$\frac{\partial^2 G}{\partial \sigma^2} \propto m^{-1} \quad .$$

It is reported (9) that H_{C1} in niobium is a second order phase transition, since there was a discontinuity in dB/dH observed, and not a discontinuity in the attenuation. The attenuation is related to the strain, but is a complex quantity. A first order phase transition must have a discontinuity in the magnetization and the attenuation measurements.

Velocity

The change in velocity as a function of temperature may also be calculated in the superconducting state (10). A velocity measurement requires the measurement of the length of the sample and its resonant frequency. The tabulated values for the linear coefficient of expansion

can only account for approximately 10% of the observed change in frequency from room temperature to liquid helium temperature in our sample. The coefficient of expansion of Nb is relatively small in the 4°K-20°K range, and this effect is neglected in this paper. The lattice itself causes a shift in frequency due to the change in lattice constant with temperature.

Elastic Modulus

The elastic moduli are functions of the lattice constants (11) and wave propagation direction in the crystal. A wave directed along the [110] direction would have an effective elastic constant for that direction. These effective elastic constants have special names and are called elastic moduli. For example, Young's modulus is the effective elastic constant that results when considering a tension along the length of a long thin rod. Young's modulus is defined as the ratio of unit stress to unit deformation. The velocity of propagation of the acoustical wave is then given by

$$v = (\mathcal{M}/\rho)^{1/2}$$

where $\mathcal{M}$ is the modulus, or effective elastic constant, ρ is the density, and v is the velocity. Since at the fundamental resonance, measured by an oscillator, the length of the rod is half the wavelength, the velocity can be calculated. Knowing the density of the material as a function of temperature then allows computation of the effective elastic constant. The elastic constants define the longitudinal modulus for different crystal directions as given below (3):

$$Y_{110} = \tfrac{1}{2}(C_{11} + C_{12} + 2C_{44})$$

$$Y_{111} = \tfrac{1}{3}(C_{11} + 2C_{12} + 4C_{44})$$

$$Y_{100} = C_{11} .$$

There is a difference between isothermal and adiabatic elastic constants; however, this difference is small at low temperatures. This research is concerned with adiabatic elastic constants only.

CHAPTER III

EXPERIMENTAL TECHNIQUE

Method In General

The experimental technique involves a capacitor transducer (12) with the sample used as one plate of the capacitor. The electronic signal is terminated in a brass electrode of approximately the same diameter as the sample and aligned coaxial with it. The electrode and cylindrical sample form a parallel plate capactior. The spacing between the electrode and sample is adjustable in order to insure sufficient driving power to convert the electrical signal in the electrode into an acoustic signal in the sample. The A-C signal in the electrode causes a varying force on the other plate of the capacitor and at the same frequency as the A-C source, when the signal is biased completely above ground. Thus, the oscillator is tuned to the resonant frequency of the rod as detected by the voltage output signal from the rod.

When the plates of this capacitor are approximately parallel, the longitudinal resonance of the rod is easily found. When the plates are not very parallel, a bending mode in the sample is excited, due to one side of the sample end being driven harder than the opposite side. If a fin is cut on the end of the sample and the electrode fit to each side of the fin, a shear wave may be excited (Figure 1). Each mode has been observed; although, the primary mode of interest in this work was the

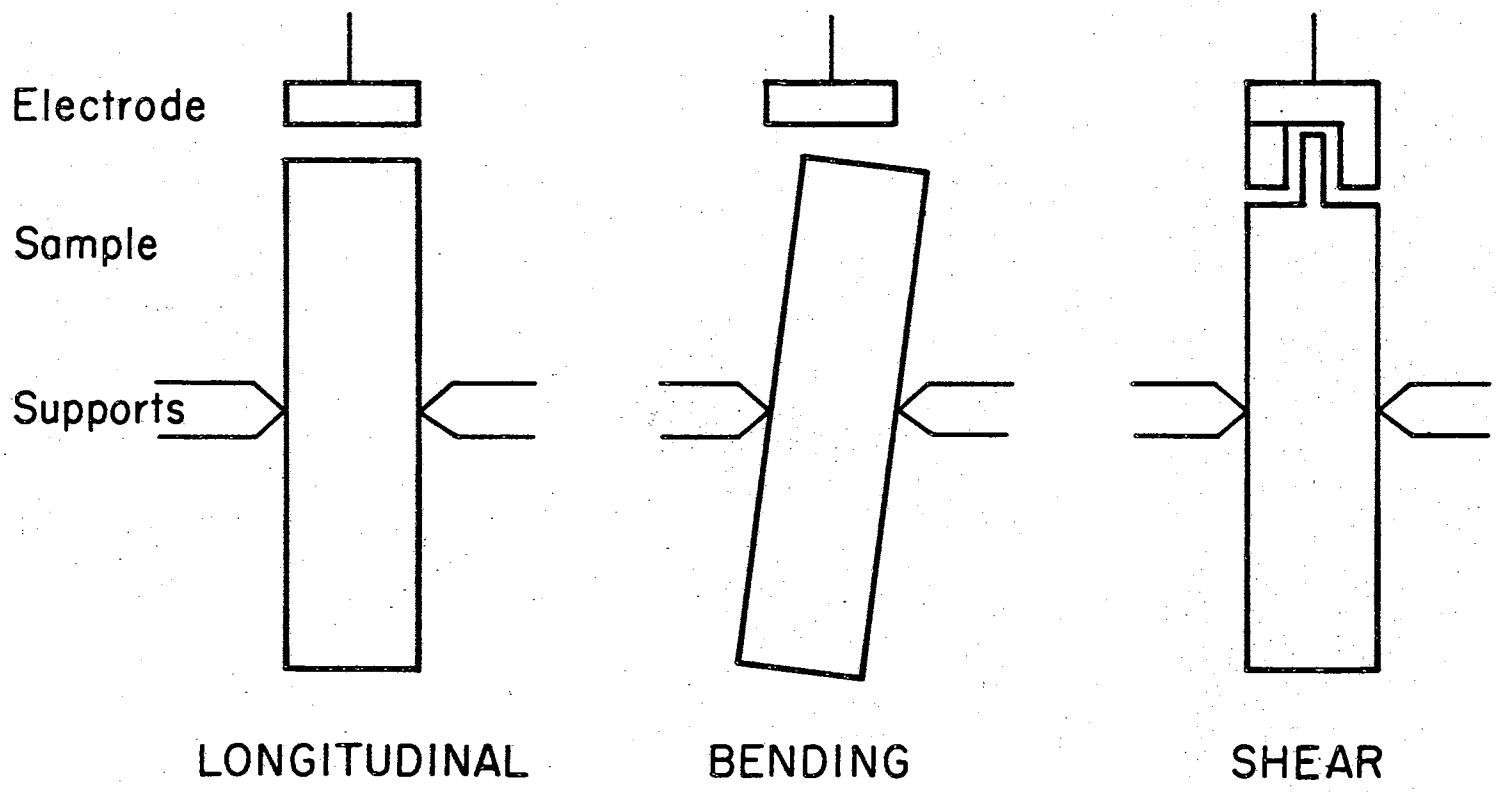

Figure 1. Excitation Modes

longitudinal resonance and Young's modulus.

The sample was clamped at its center, because this was the nodal plane for the fundamental resonance. Since a nodal plane experiences no motion at resonance, clamping at this position interfered in a minimum way with the attenuation measurement. The resonant frequency was the actual measurable quantity with its change directly proportional to the change in modulus,

$$f = v/\lambda = v/2l = \sqrt{m/\rho}\,/\,2l$$

where f = frequency, v = velocity, l = length of sample, λ = wavelength, m = modulus, and ρ = density. It is shown in Appendix B that

$$\frac{\Delta m}{m} \approx 2\,\frac{\Delta f}{f} \quad .$$

Therefore, the accuracy in the modulus changes depends only on the accuracy of the frequency.

Control Experiments

In order to have accurate measurements, all possible influencial factors must be investigated. In this experiment there were several important variables to consider. A method of measuring the temperature accurately was the first project. A thermocouple of gold-cobalt versus silver-gold was used. This combination gives a high thermoelectric power, i.e. a large change in voltage per degree change in temperature. Since calibration tables for this thermocouple were not readily available, a calibration was necessary. The relation of voltage to temperature within a third order approximation was sufficient for temperature readings of 0.1°K.

$$EMF = \alpha T + \beta T^2 + \gamma T^3 \quad .$$

Using three known temperatures as calibration points, three equations with three unknowns were obtained. These equations were used to solve

for α, β, and γ. With these constants known ($\alpha \approx 10^{-2}$, $\beta \approx 10^{-5}$, $\gamma \approx 10^{-7}$), the computer was able to calculate the voltages for any desired temperature. The program for the computer is included in Appendix A.

Clamping the specimen effected the measurement of the attenuation and velocity and was investigated seperately. Two methods of clamping were devised. One way was to clamp the specimen between two wires at the center nodal plane. Those wires served as an electrical contact and ground for the specimen. It proved to be very difficult to apply the correct tension in these fine wires in order to both support the specimen and not break the wires upon thermal contraction at low temperatures. A successful configuration used a nylon monofilament with a fine wire coiled around it to serve as a ground connection. A small groove was cut around the center of the specimen to facilitate the assembly procedure. The rod was so loosely suspended now that the slightest vibration in the building would cause the entire rod to move. This motion of the specimen made measurements difficult to obtain.

An alternate method comprised of four needle-pin supports proved to be much more easily assembled and more reliable at low temperatures. With the groove cut around the perimeter of the nodal plane, the needle points allowed the specimen to hang relatively free on the four contact points. The pressure that the pins applied on the sample caused a change in the attenuation, as seen in Figure 2. The minimum pin pressure was sought for each time. It was easier to achieve this optimum pin pressure than to gamble with the wire suspension. The position of clamping is, as would be expected, an optimum in attenuation on the nodal plane (Figure 3).

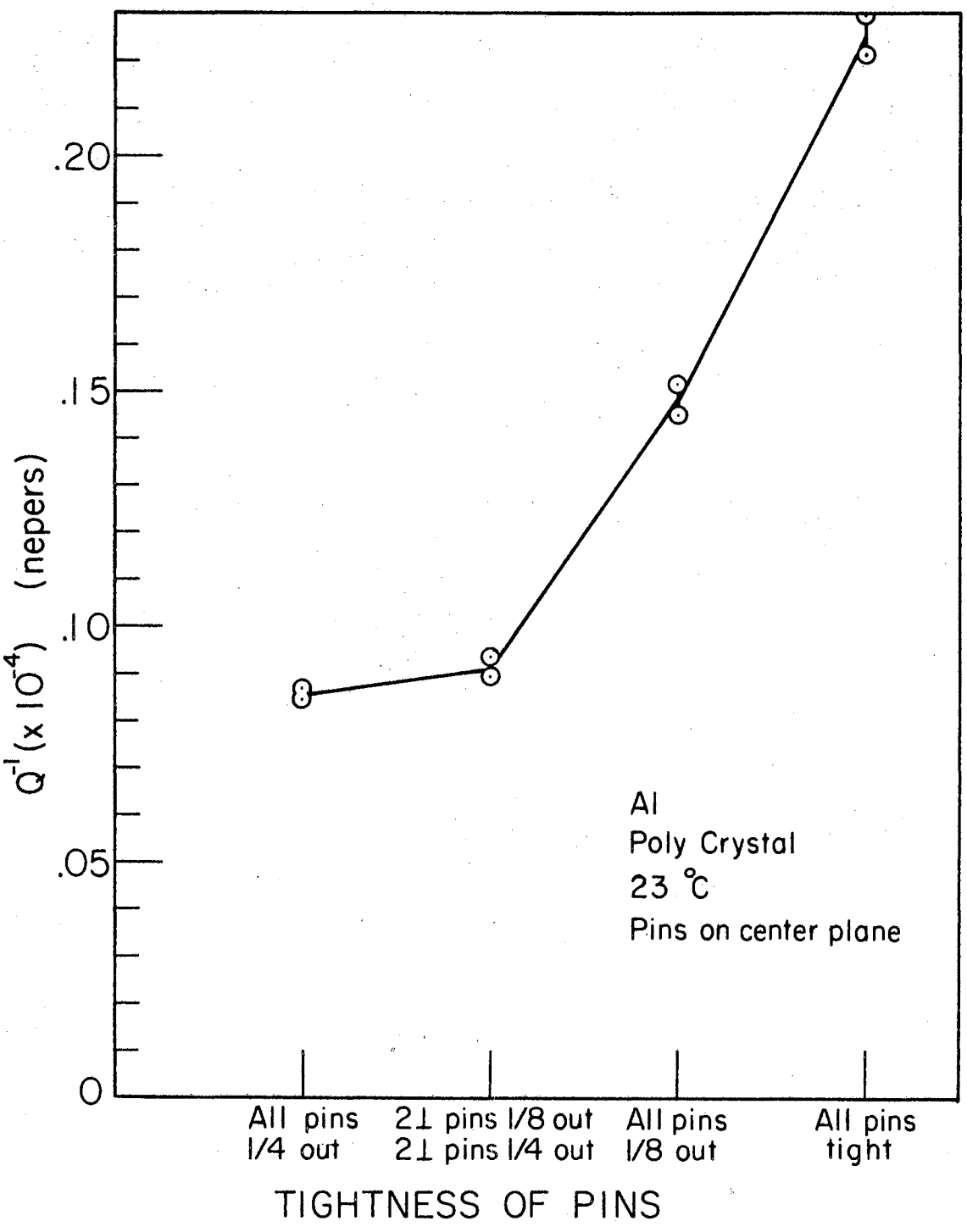

Figure 2. Pin Pressure

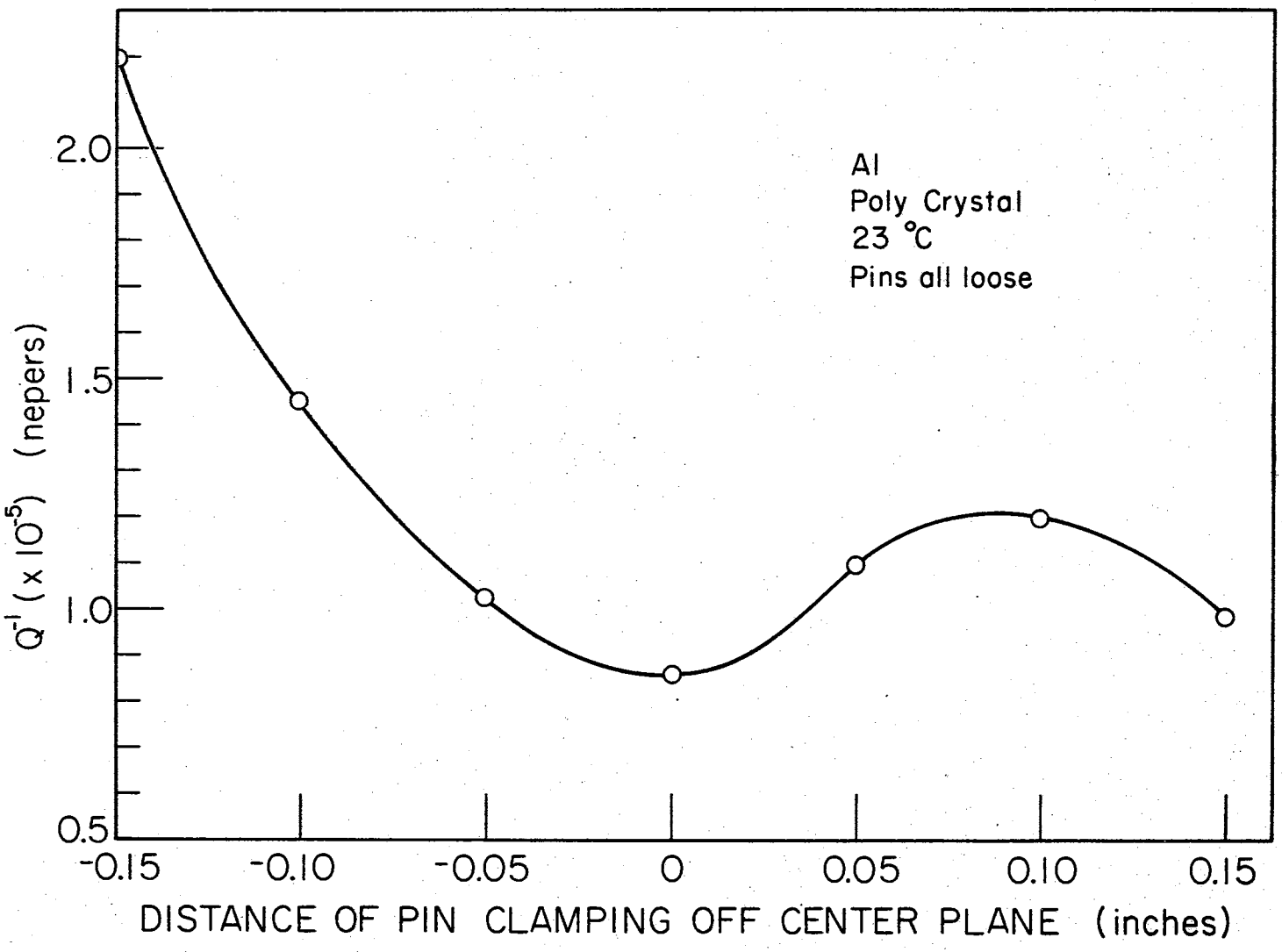

Figure 3. Pin Position

The amplitude dependence of the attenuation was investigated (10). There were two ways to adjust this variable: 1) by the oscillator output voltage adjustment, and 2) by the electrode spacing of the capacitor plates. When the electrode spacing becomes too small, the resonant frequency of the rod gradually increases, as does the attenuation. This effect is corrected by increasing the spacing in the capacitor by backing the electrode away until any further adjustment would not change the resonant frequency. Any spacing greater than this critical spacing has no effect on the attenuation. The oscillator amplitude proved to have no effect in the normal state. In the superconducting state, however, an increase in amplitude slightly lowered the resonant frequency, but did not effect the attenuation. This is shown graphically in Figures 4 and 5.

A check was run on the resonant frequency of the poly crystalline rod to make sure that this resonance was the longitudinal one. The resonant frequency should have a harmonic approximately double the fundamental. It will be slightly less than double due to dispersion. It should be noted that the bending mode does not simply double. By checking the resonances between the fundamental and the first harmonic, the type of resonance can be determined. The differences between the bending harmonics vary in a smooth fashion. For the bending mode a plot of $\Delta f = f_{n+1} - f_n$ versus f should yield a smooth half parabola type curve.

As stated by others (13) the ambient pressure also effects the attenuation measurements. As long as the pressure is kept below 500 microns, there is no pressure dependence. Above that value, the attenuation increases. Also, surface dirt on the sample causes a slight

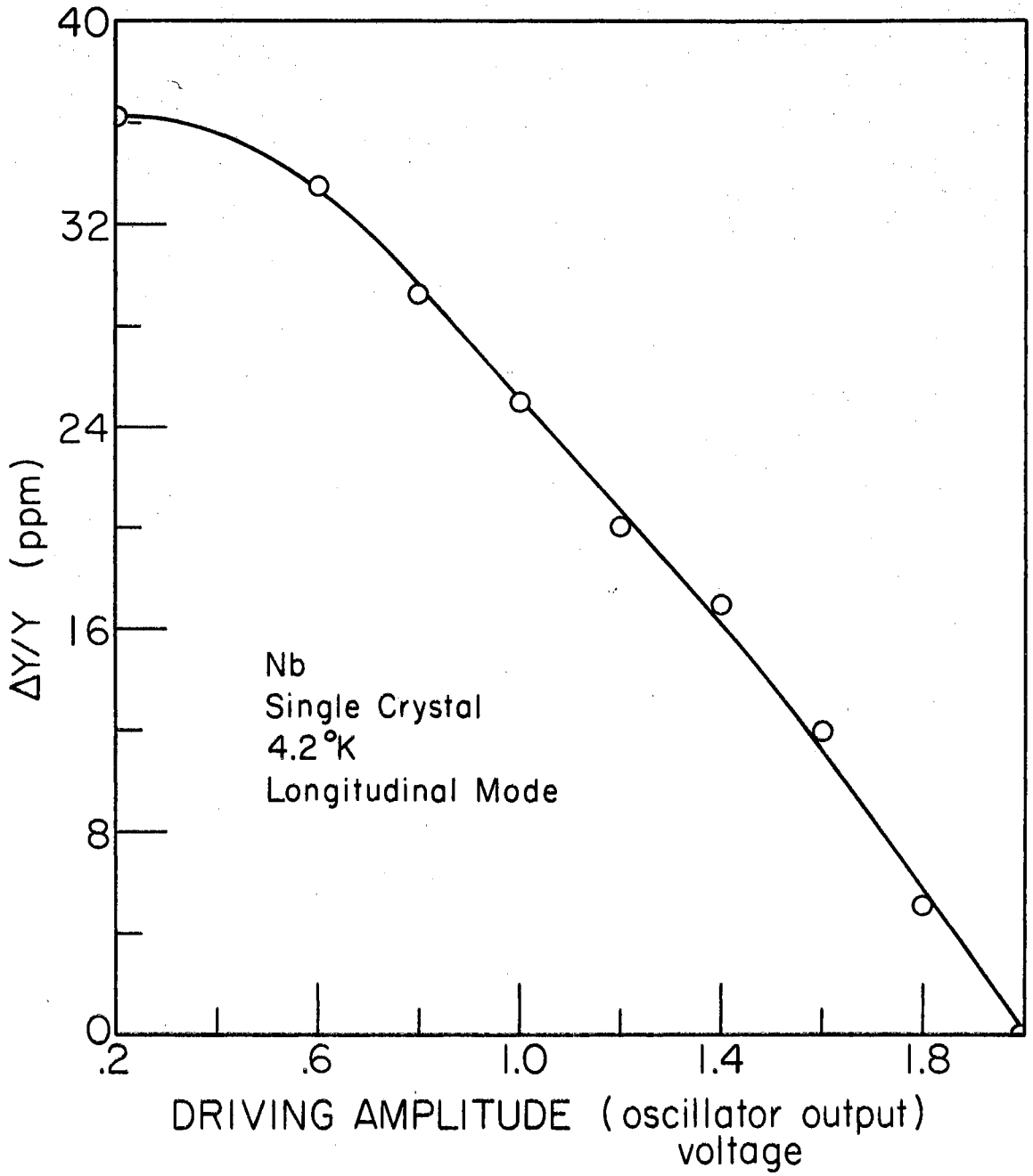

Figure 4. Young's Modulus Amplitude Dependence

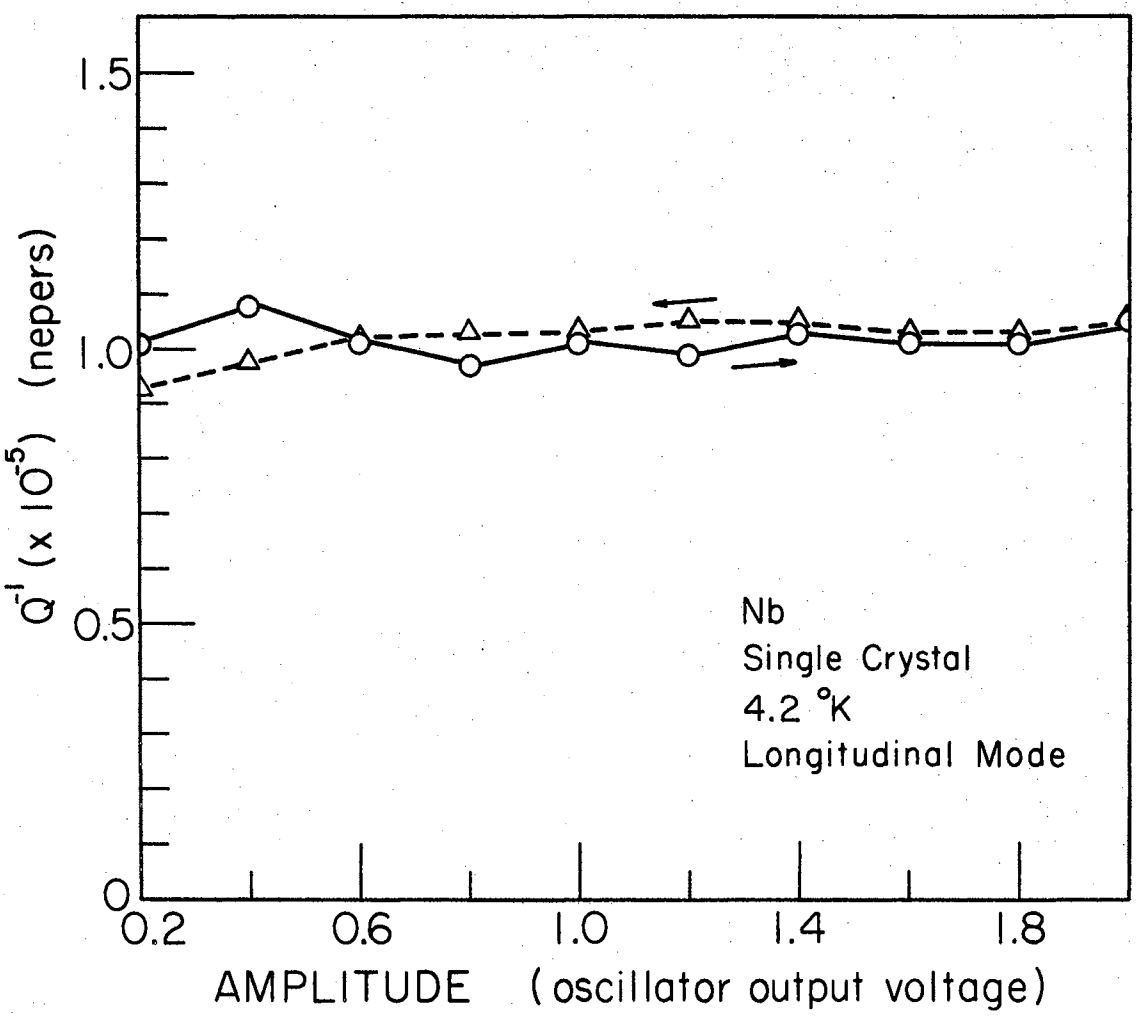

Figure 5. Attenuation Amplitude Dependence

increase in attenuation.

The effects of an external magnetic field were also investigated (14). The magnet used was calibrated with a Hall probe and gauss meter. The residual field was about 50 gauss. Four inch cylindrical pole faces with a four inch gap were used. The field was applied perpendicular to the sample's cylindrical axis. The field varied approximately 50 gauss from the center to one end of the sample and only a few gauss across its width out of a 2000 gauss field.

Apparatus and Measurements

The block diagram in Figure 6 gives an overall view into the instrumentation required for these measurements. The origin of the electronic signal is an oscillator, a General Radio Frequency Synthesizer, Type 1161 - A. It operates from 0 - 100 kHz and has an accuracy of nine significant figures in the frequency. The output voltage of the oscillator is 0 - 2.2 vpp. The signal next sees a 50:1 step-up transformer which increases the maximum driving voltage to 110 vpp. A microswitch is added to the signal line in order to be able to cut off the driving signal when desired. The divider network channels the incoming signal into the sample and directs the outgoing signal from the sample onto the F-M detector. The divider network and F-M detector were designed and built by J. F. Guess and G. B. Thurston (15) for a similar purpose in the audible frequency range. If the driving signal is referenced about the ground voltage, then the input frequency is doubled between the electrode and the sample. Thus, a driving frequency of one-half the resonance of the rod is required. However, if the input signal is referenced completely above, or below, ground voltage, then

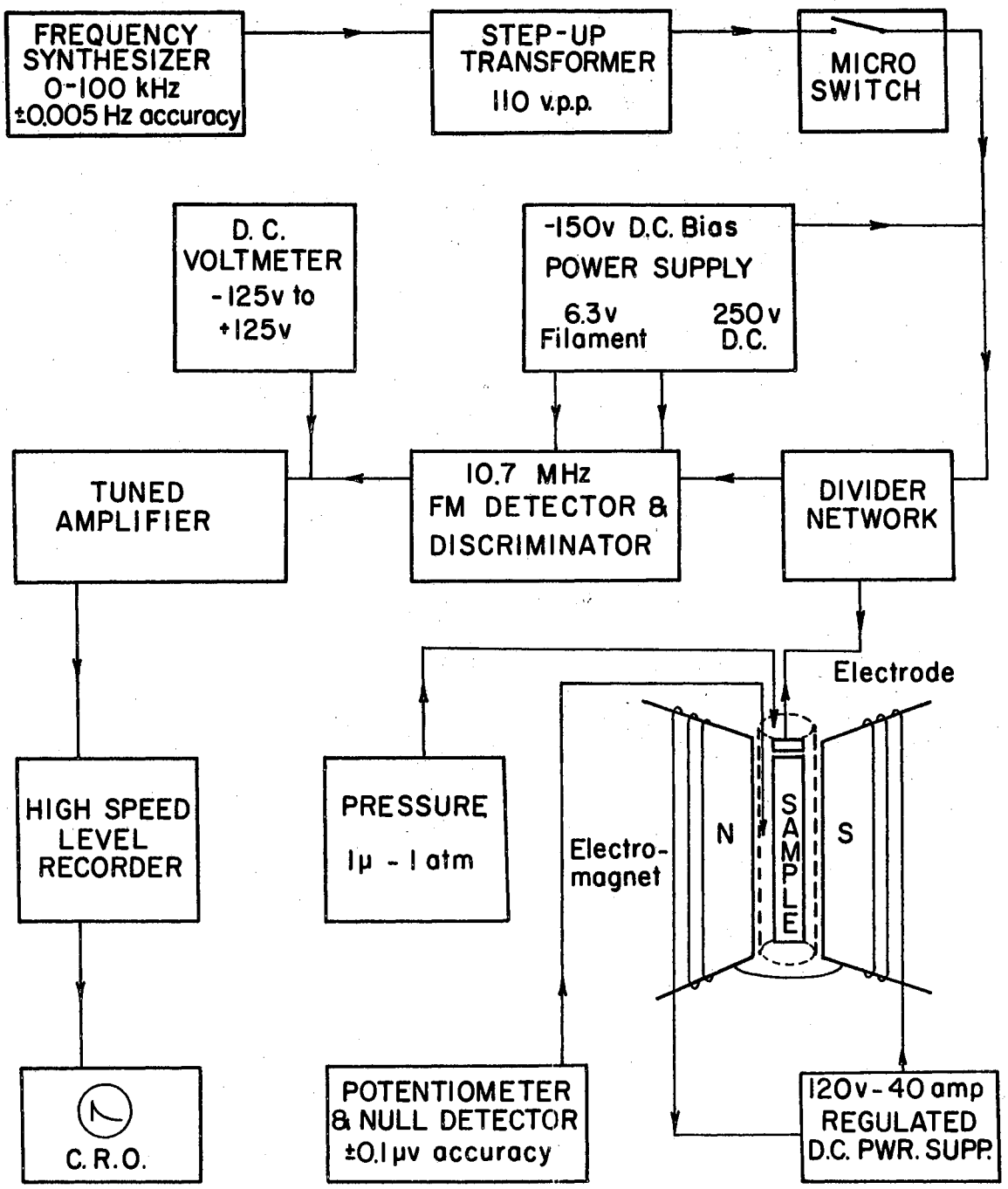

Figure 6. Block Diagram

the frequency is not doubled in the capacitor formed by the sample. The motion of the end of the sample due to the capacitive driving force causes a change in capacitance of the capacitor formed by the electrode and sample. This capacitor is in parallel with the tank circuit of the 10.7 MHz F-M detector and modulates the detector about the 10.7 MHz center frequency. This center frequency is adjustable by a variable capacitor in the tank circuit. The modulation frequency is generally around 40 kHz. The F-M detector feeds the signal into a discriminator which picks out the resonant frequency of the rod. When the resonant frequency is centered correctly, a D.C. voltmeter will null at zero volts between the discriminator output and ground. This 40 kHz signal is then amplified by means of a tuned amplifier and recorded on a high speed level recorder, as well as being monitored on an oscilloscope.

The attenuation can be measured in two ways. The Q may be measured directly, $f/\Delta f$, by observing the frequency at the 3 db points (bandwidth) on each side of the resonant frequency. This method is preferable when the Q is low and the resonant frequency is not well defined. The Q is a measure of the total energy in the sample as compared to the decrease in energy per cycle dissipated by the sample. The second method is called the free decay method. In this method the signal that drives the sample at its resonance is cut off via the micro-switch. The rate of decay of the energy is used to determine the attenuation. This decay of output signal is exponential, but when recorded on a logarithmic recorder as a function of time, it gives the time constant, or decay time, directly by the slope of a straight line. This decay time is related to the Q of the sample directly by

$$Q = \pi f \tau$$

where f is the frequency and τ the decay time. One usually talks about $\eta = Q^{-1}$, since η is proportional to the attenuation. Therefore,

$$\eta = (\#db\ decay)/8.68\pi f\tau \quad nepers\ .$$

The temperature was measured by a Au - Co versus Ag - Au thermocouple. A Leeds and Northrup Potentiometer, Type K-4 was used with an electronic D-C Null Detector. The potentiometer is accurate to 0.1μV, giving a temperature accuracy of better than 0.1°K. As mentioned earlier, the thermocouple was often calibrated to insure accuracy.

The pressure was measured by a Kinney Vacuum Gauge, Model KTG-3. This was calibrated with a Kinney McLeod Gauge, Type TDI-MK III below 100 microns of pressure.

The sample was suspended on four pin supports inside a brass can, so that the sample chamber could be evacuated. The sample chamber (see figure 7) contained the electrode, the sample, the temperature thermocouple, and a resistor for heating the chamber. The chamber was surrounded by the conventional double dewar system for liquid helium. Then the entire assembly was injected between the pole faces of the electromagnet. The magnetic field could be read within 2%.

Niobium crystals are body centered cubic. Both the single crystal and poly crystalline samples were obtained from Materials Research Corporation, Orangebury, New York. A typical mass spectroscopic analysis was included with each sample. 100 ppm of tantalum was reported with only a few ppm, or less, of all other impurities. The single crystal is oriented along the (117) direction. The single crystal is 1.725 inches long and .25 inch in diameter. The poly crystal is 1.600 inches long and .25 inch in diameter. The resonant frequency of the single crystal was about 45 kHz, and that of the poly crystal was about 40 kHz.

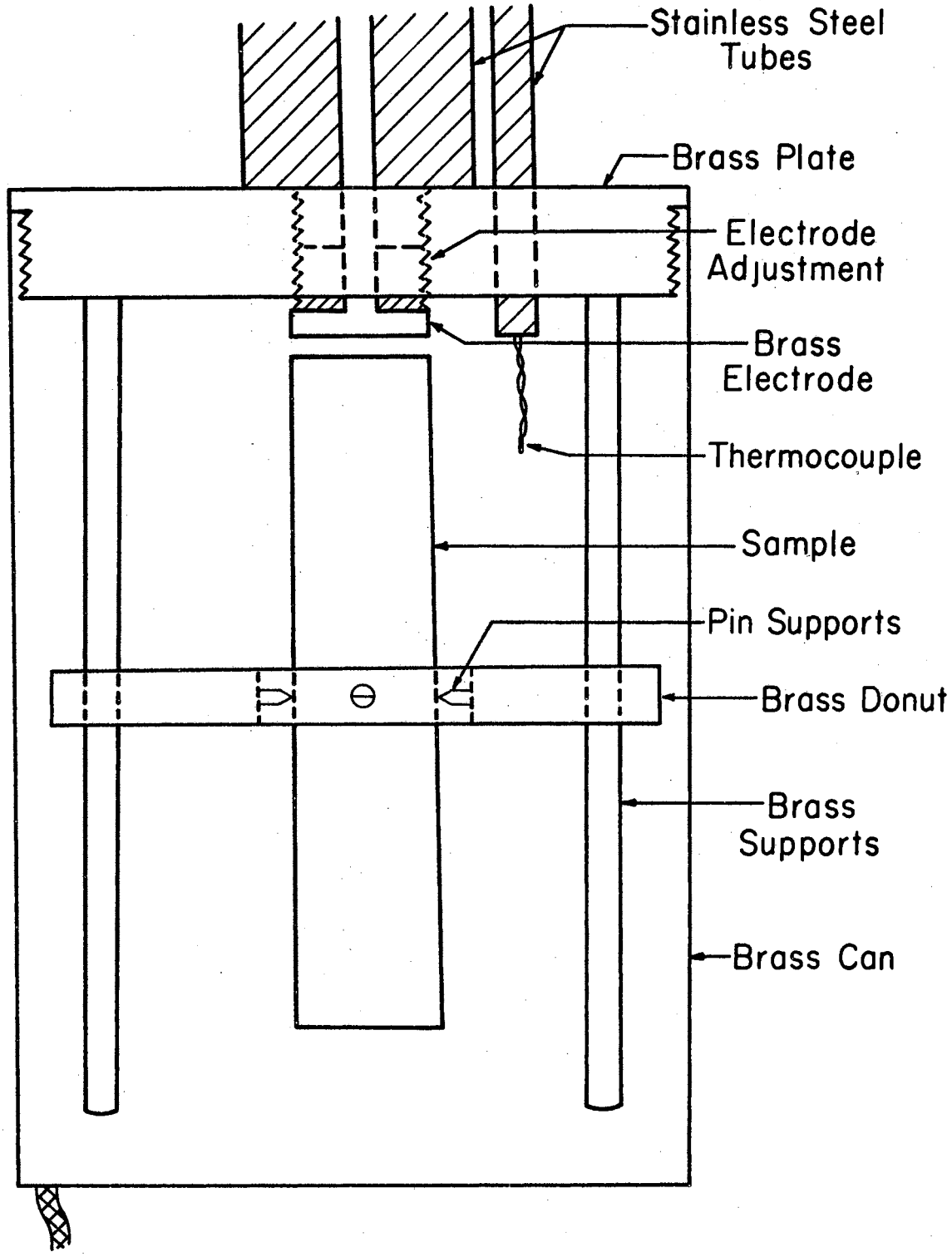

Figure 7. Sample Chamber

CHAPTER IV

RESULTS

The results of this work can be classified into the following four groups:

A. Resonances,

B. Temperature drift measurements,

C. Attenuation measurements as a function of magnetic field, and

D. Changes in Young's modulus as a function of magnetic field.

Resonances

The poly crystal resonances were found at 41,438.4 hz and 81,978.2 hz at nitrogen temperature. This shows a 2.17% dispersion at the first harmonic.

In the single crystal two resonances were found close to the expected frequency. They were approximately 46.5 kHz and 46.7 kHz at liquid helium temperature and approximately equal magnitudes. This led to an investigation of a possible bending mode, presupposing that the sample was not alligned well. This did not turn out to be the case. Many small resonances were found, but only a few had an attenuation coefficient similar to the original two (Table 1 and Figure 8).

However, it was found that many of the resonances appeared in

TABLE I

RESONANT FREQUENCIES

Nb Single Crystal at Nitrogen Temperature

Frequency (Hz)	Comments
10,125.	large
10,481.	small
11,962.	large; decay time about 1 second
13,080.	small
15,665.	small
16,681.	small
17,010.	small
19,955.	large
20,938.	large
25,260.	large
27,585.02	very large; decay time about 30 seconds
30,855.	small
33,562.	small
36,305.	small
37,620.	small
39,310.	small
41,420.	large
45,250.	medium
46,229.18	f_{110}; decay time about 10 seconds
46,374.08	f_{111}; decay time about 10 seconds
48,040.93	large
49,455.	small
50,200.	small
51,840.	small
59,580.	small
69,850.5	large
75,170.	small
75,660.	small
78,520.	small
79,328.	small
90,172.0	large
99,235.	small

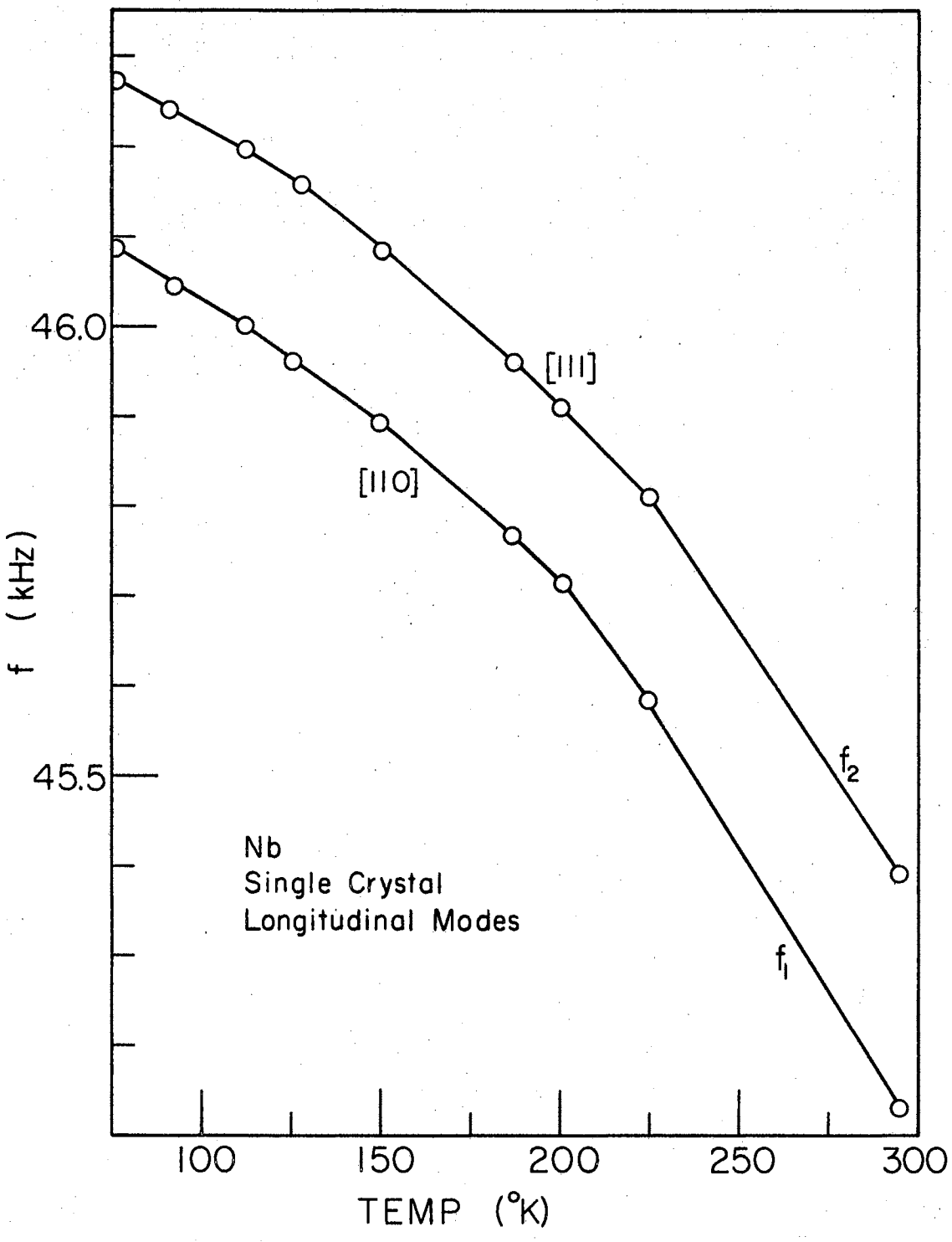

Figure 8. Resonances in Nb

closely group pairs. This brings about a theory that the crystal itself caused the two resonances. Since the crystal is oriented in a (117) direction, this proves to be possible. The [771] direction is not an easy direction in which to propagate an acoustical wave. However, the pure mode directions, [001], [111], and [110], are easy directions in which acoustical propagation occurs. The [110] is closest to the [771], and the [111] is the next closest of these three pure modes. The wave finds it easier to split and propagate partly along the [110] and partly along the [111] than to propagate in the [771] direction (see Figure 9). This is understandable for high frequencies, but rather odd for these low frequencies. However, it appears to be what is happening. From published tables (15)

$$C_{11} = 1920,\ C_{12} = 1340,\ C_{44} = 568 \quad .$$

Therefore, the longitudinal effective elastic constants are

$$m_{110} = [110]_L = \tfrac{1}{2}(C_{11} + C_{12} + 2C_{44}) = 2198$$

and

$$m_{111} = [111]_L = \tfrac{1}{3}(C_{11} + 2C_{12} + 4C_{44}) = 2291.$$

Therefore,

$$m_{110}/m_{111} = 0.96 \quad .$$

Since

$$v = f\lambda = \sqrt{m/\rho} \quad ,$$

then

$$(f_1/f_2)^2 = m_1/m_2 \quad ,$$

or

$$(f_{110}/f_{111})^2 = (45.13\,kHz/45.39\,kHz)^2 = 0.99 \quad .$$

This is in reasonable agreement. The [110] direction should have the lower frequency, since its modulus is less than that of the [111] direction.

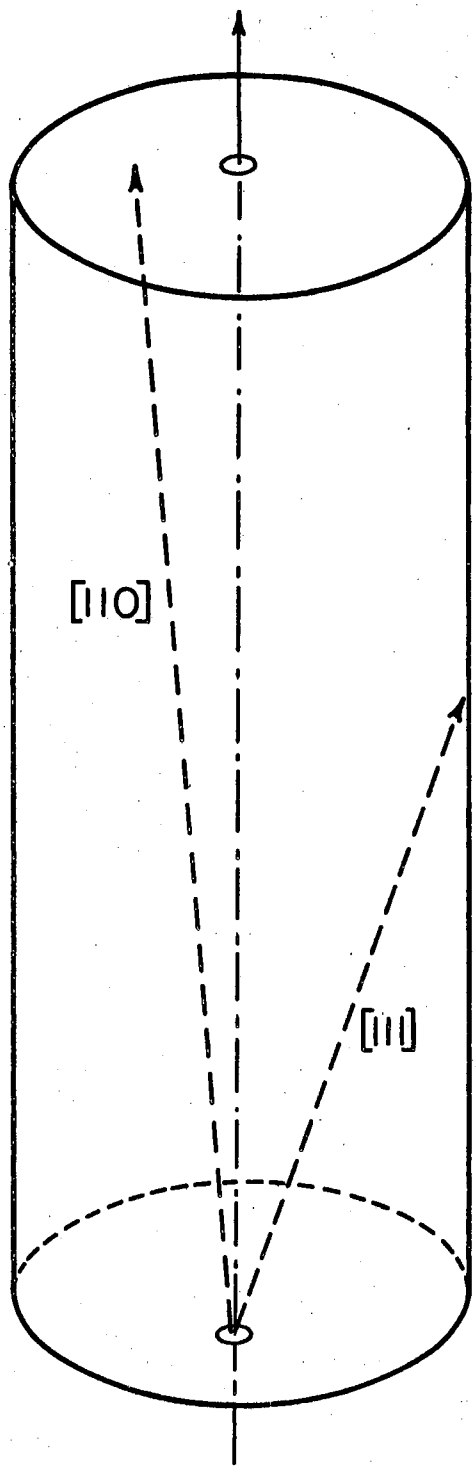

Figure 9. Nb Single Crystal

Temperature

This area is not restricted to the superconducting region, but it includes a large temperature range for comparison. Figure 10 shows the Bordoni Peak (17) in the single crystal of Nb. Figure 11 shows the changes in Young's modulus as a function of temperature. A relaxation process is observed around 40°K. Since this temperature is hard to attain and this is not the primary concern of this paper, no further investigation was conducted. Note, however, that the relaxation process does correspond to the second peak on the Bordoni graph. The third graph shows the changes in modulus for the poly crystalline Nb sample as a function of temperature. No relaxation process is seen in Figure 12.

Attenuation

The attenuation measurements were first made in the normal state at nitrogen temperature in order to show the normal magnetic effect. Any dependence observed in the normal state must be subtracted from the superconducting effect to find the dependence due only to the superconducting state. The single crystal showed no magnetic effect in the normal state, i.e., the niobium single crystal attenuation is independent of field up to 2700 oersted (Figure 13). The poly crystalline sample showed a very small magnetic effect in the attenuation measurement. This normal state effect was small enough to be neglected in the superconducting measurements (Figure 14).

The superconducting results proved to be interesting. The poly crystalline sample (Figure 15) recorded a spike in the attenuation at 800 oersteds, which is believed to be H_{C1}. The attenuation changed

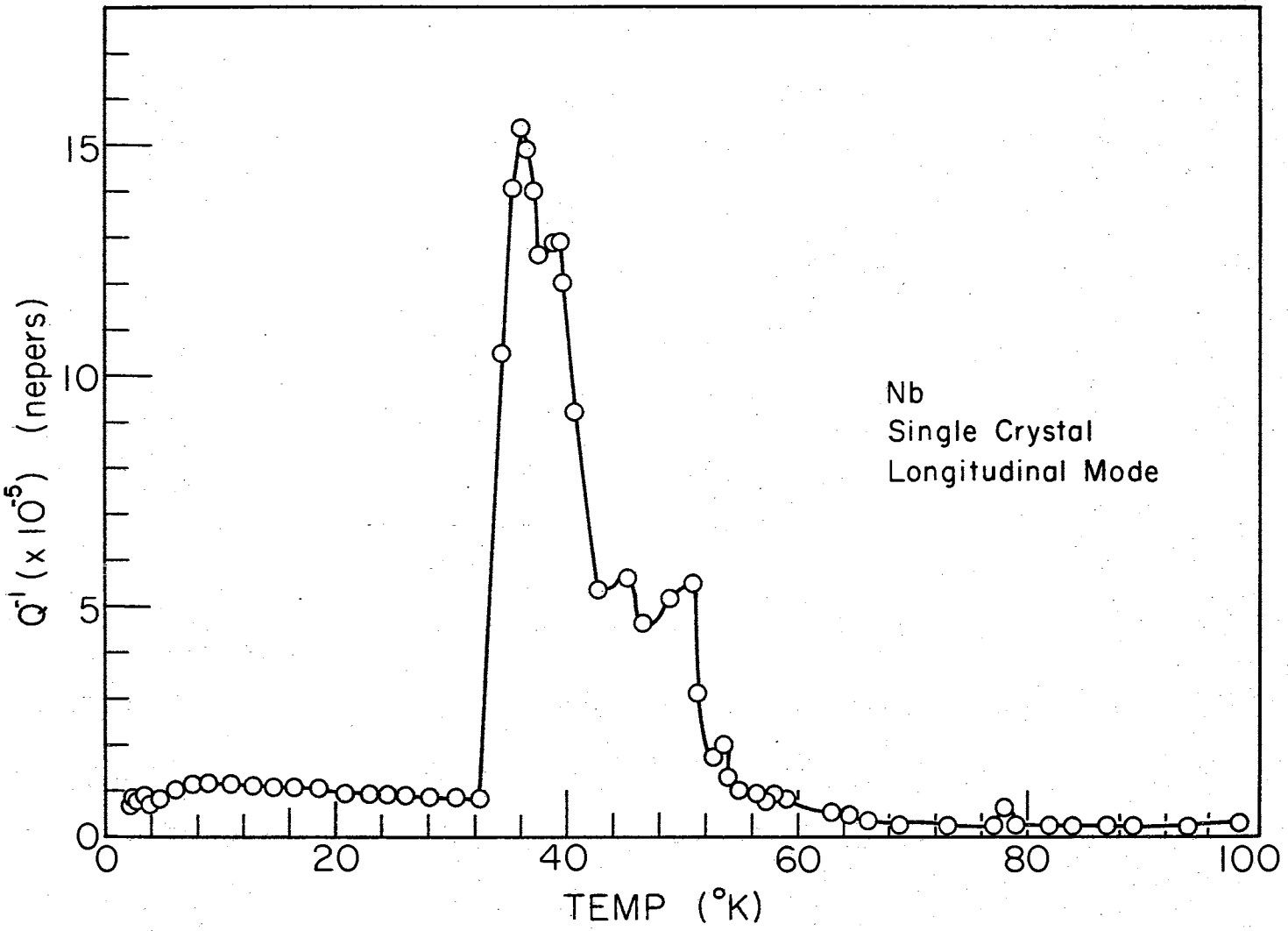

Figure 10. Bordoni Peak

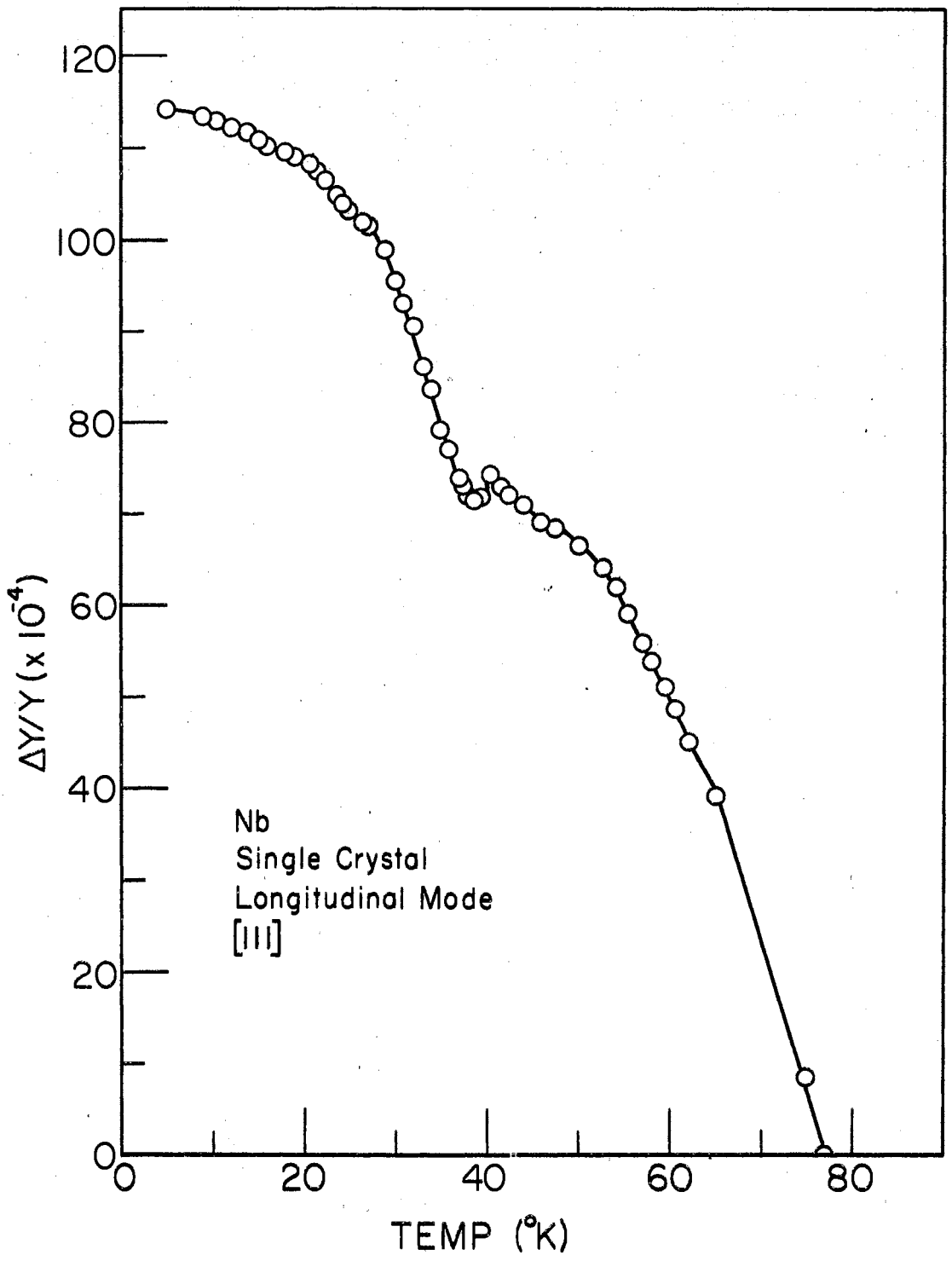

Figure 11. Relaxation Process

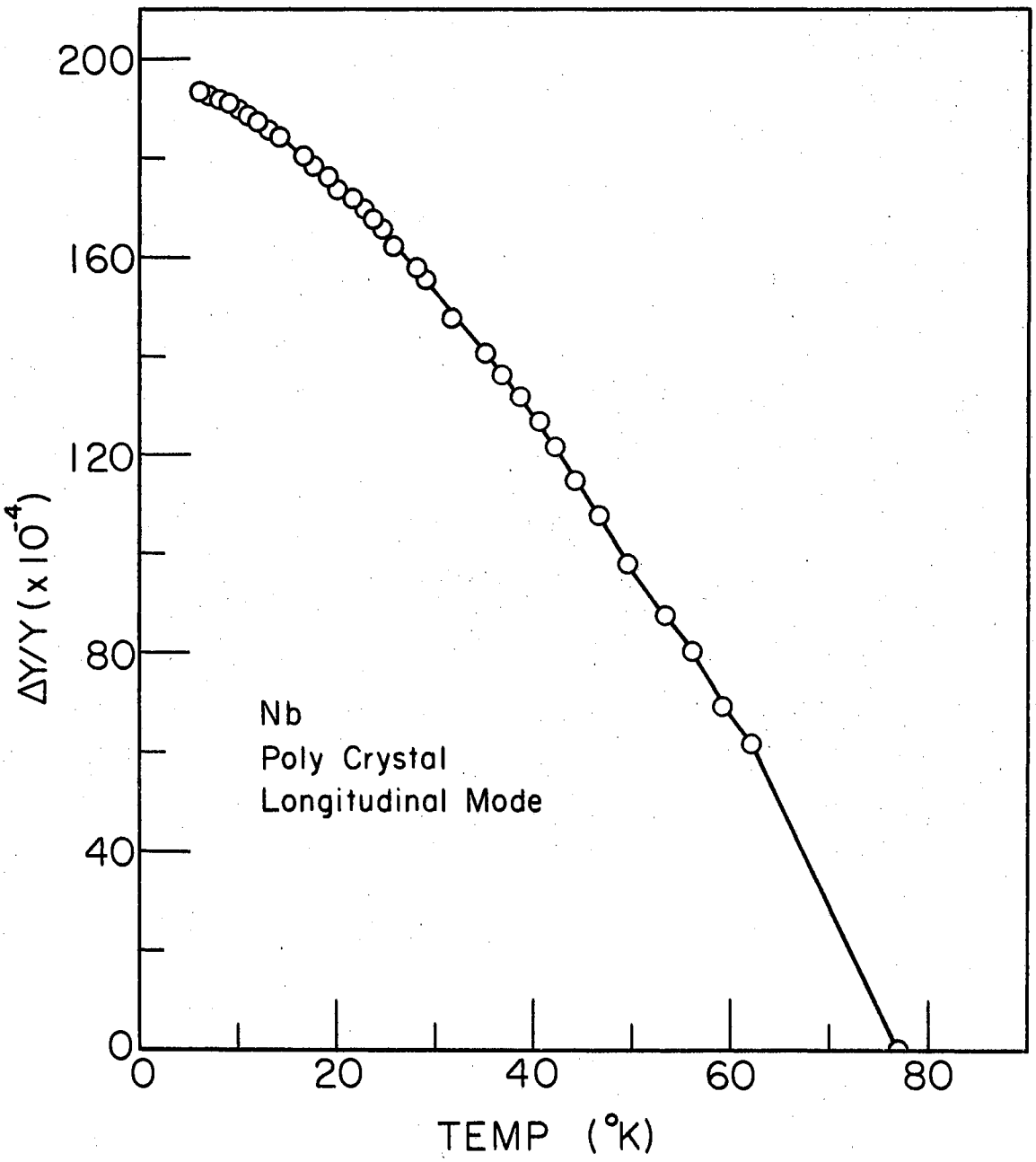

Figure 12. Nb Poly Crystal

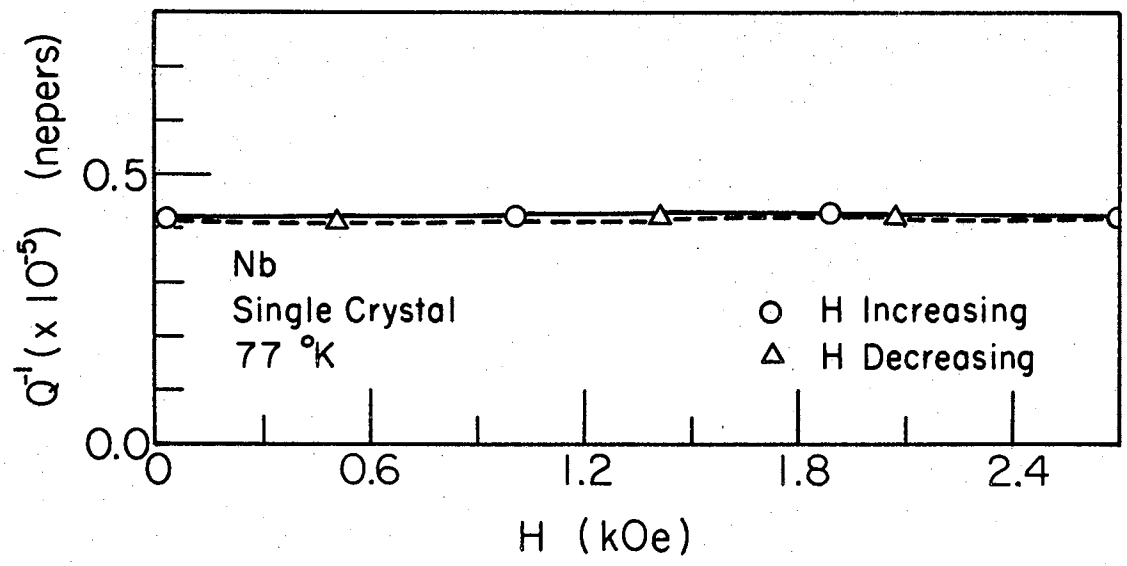

Figure 13. Single Attenuation in Normal State

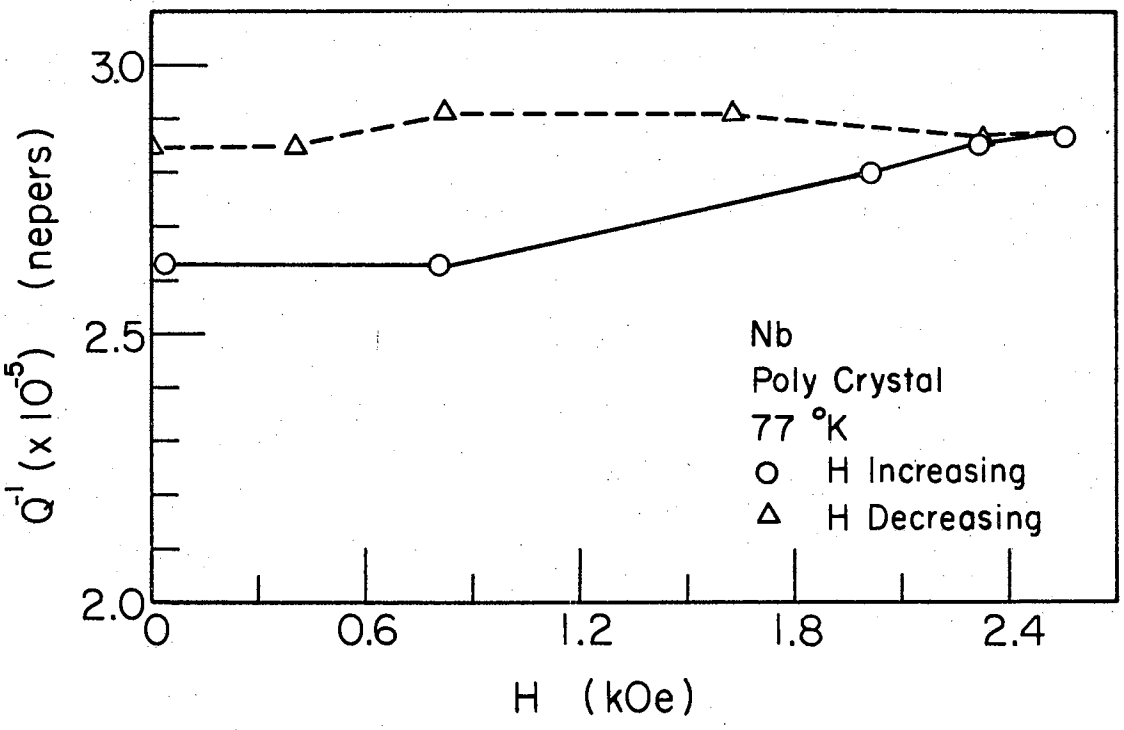

Figure 14. Poly Attenuation in Normal State

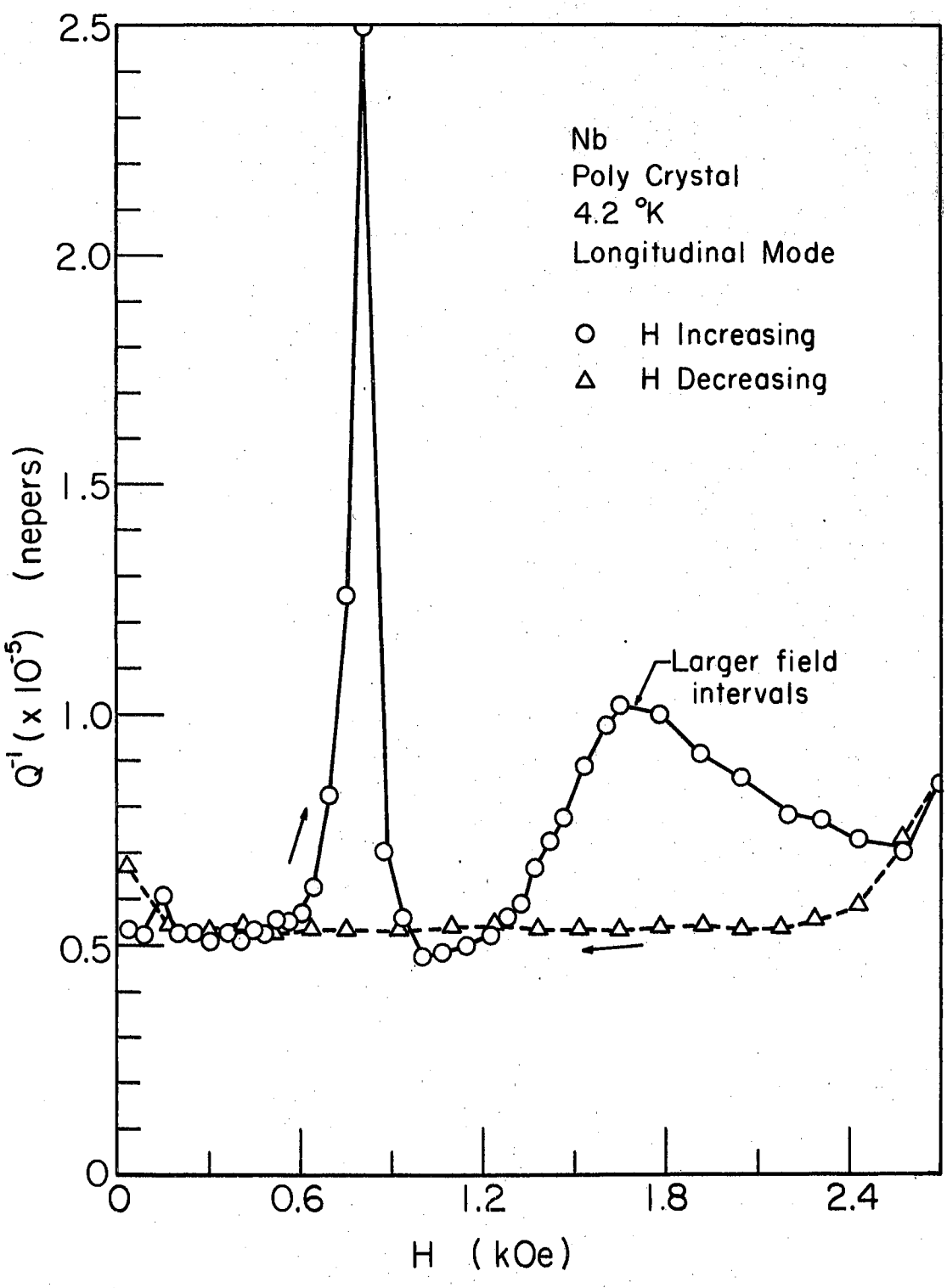

Figure 15. Poly Attenuation

slope at 1700 oersteds and again at 2600 oersteds. Although only one point indicates this last change in slope, this occurs at a value of magnetic field believed to be H_{C2}. The first change in slope occurs when the field intervals were increased. This should be repeated when equal field and time intervals between all measurements can be attained to insure no long relaxation process is connected with the changing field. Neuringer and Shapira (18) report that the slower changes in field reduce the number of flux jumps. The single crystal [110] data is somewhat similar (Figure 16). A spike in the attenuation occurs at 750 oersteds, believed to be indicative of H_{C1}. This is followed by a generally positive slope up to 2000 oersteds. The bumps in this part of the graph are believed to be representative of flux penetrations. The negative slope in the higher field region corresponds to the poly crystalline data. The single crystal [111] data is odd, because the spikes in the attenuation occur at 400 and 1000 oersteds. This oddity may be explained, since the [111] direction is nearly 45° to the [771] direction, causing the [111] propagation to be partly shear in nature. All field runs in the superconducting state were made after raising the temperature and letting the sample return to the normal state in order to allow any trapped flux to be released, unless the run is labeled 2nd.

It should also be noted that the decay time measurement in the region of H_{C1}, or the spike, is unusual, since a double slope is seen. However, it is not a high attenuation process followed by a lower attenuation process. It is just the opposite, i.e., a low attenuation is interupted by a high attenuation. Since on both sides of this unusual measurements at H_{C1} the attenuation measurements are very uniform and indicate a single relaxation process, this phenomenon cannot be attribu-

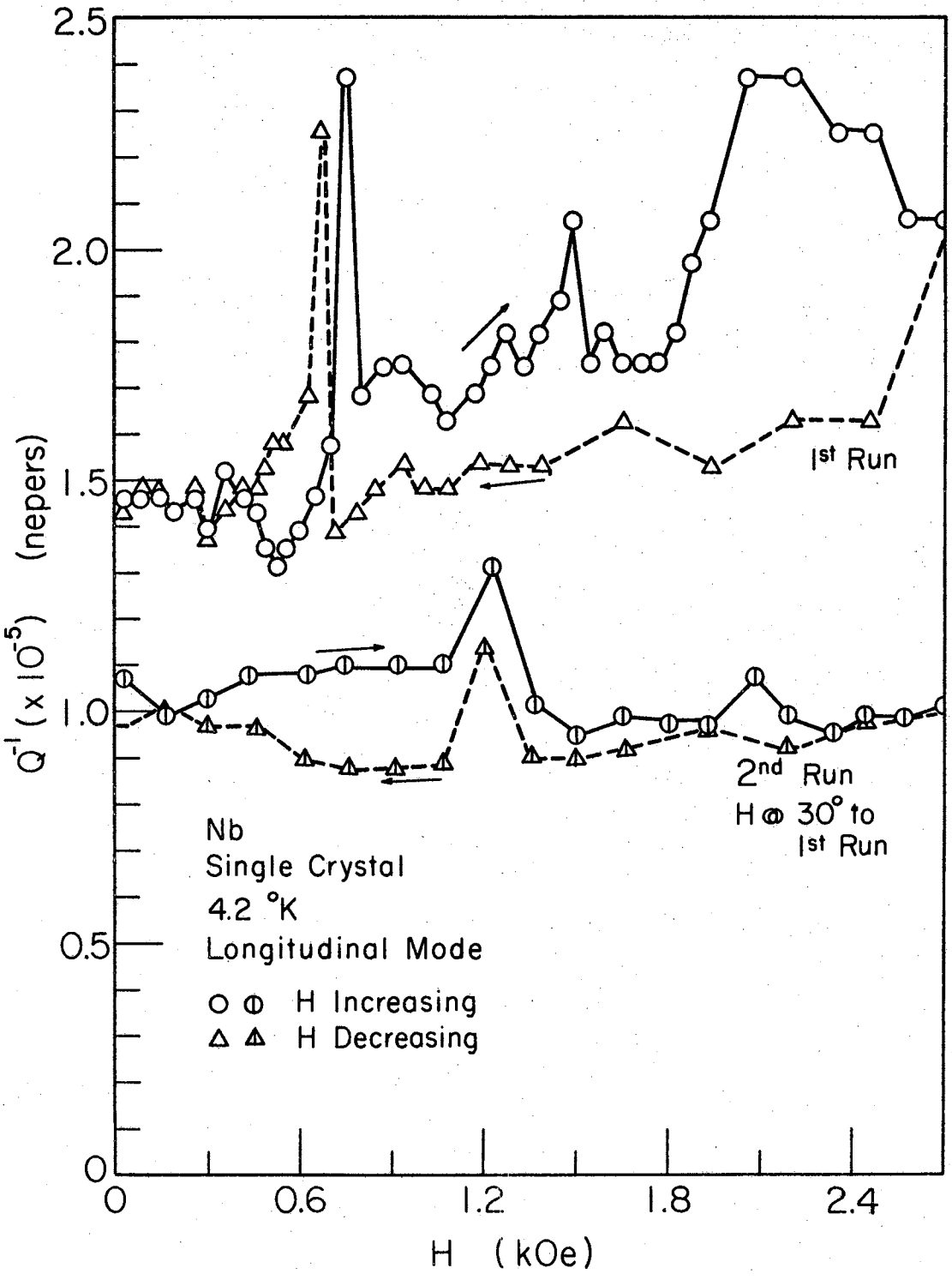

Figure 16. Single Attenuation [110]

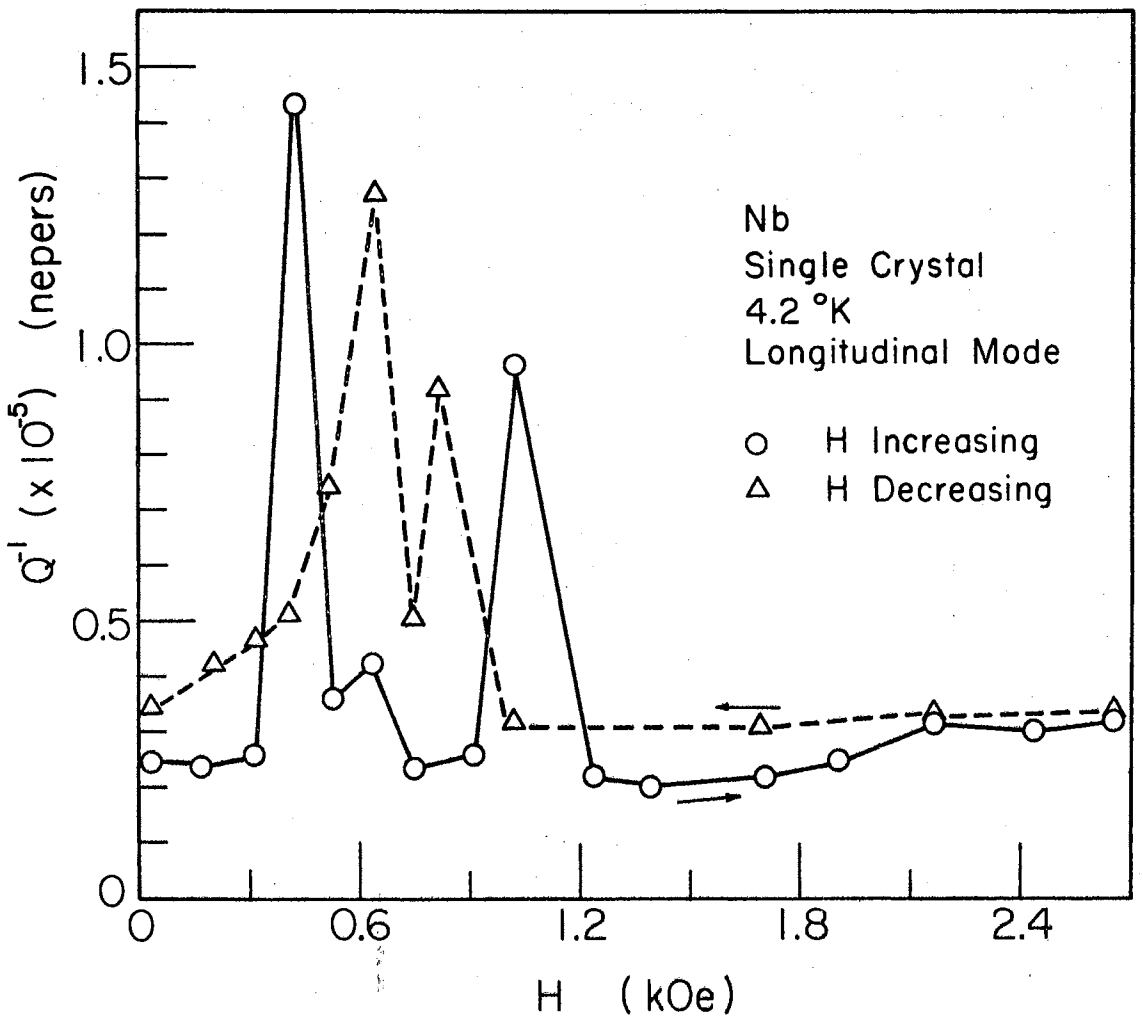

Figure 17. Single Attenuation [111]

ted to the recording apparatus. This oddity is left unexplained.

Young's Modulus

As in the attenuation measurements, the Young's modulus measurements were performed at nitrogen temperature to recognize any background effect of the normal state which must be substracted from the superconducting measurements to see the true superconducting effect. As before, no appreciable magnetic effect was recorded in Young's modulus for the normal state in either the single crystal or poly crystalline samples (Figures 18 and 19).

The superconducting data for the poly crystalline specimen indicates a discontinuity in the modulus at 800 oersteds, believed to be H_{C1}. A change in slope is also indicated at 1600 oersteds. H_{C2} is possibly not reached as implied by this data, since the normal state should show no further change in modulus. The single crystal [110] data also shows a discontinuity in the modulus at 800 oersteds, H_{C1} (Figure 21). This is followed by a generally positive slope with possible flux penetration bumps superimposed on it. Again H_{C2} is not believed to be reached. The [111] direction data is different than that above. Minima in the modulus occur at 400 and 1000 oersteds with a large maximum at 600 oersteds. This corresponds with the attenuation data and is believed to be due to the partly shear mode. The [110] direction in the single crystal and the poly crystalline sample are always perpendicular to the magnetic field. The [111] direction is only perpendicular to the field for two possible orientations of the sample with the field. For other orientations it may be off 45° with respect to the field. This orientation was not known for each run.

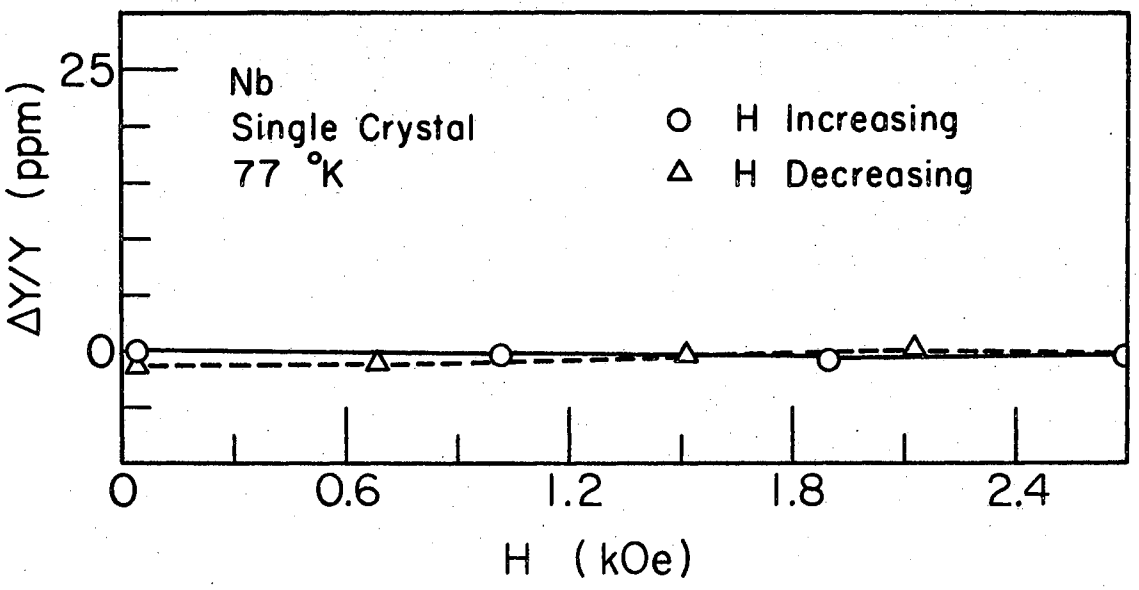

Figure 18. Single Modulus in Normal State

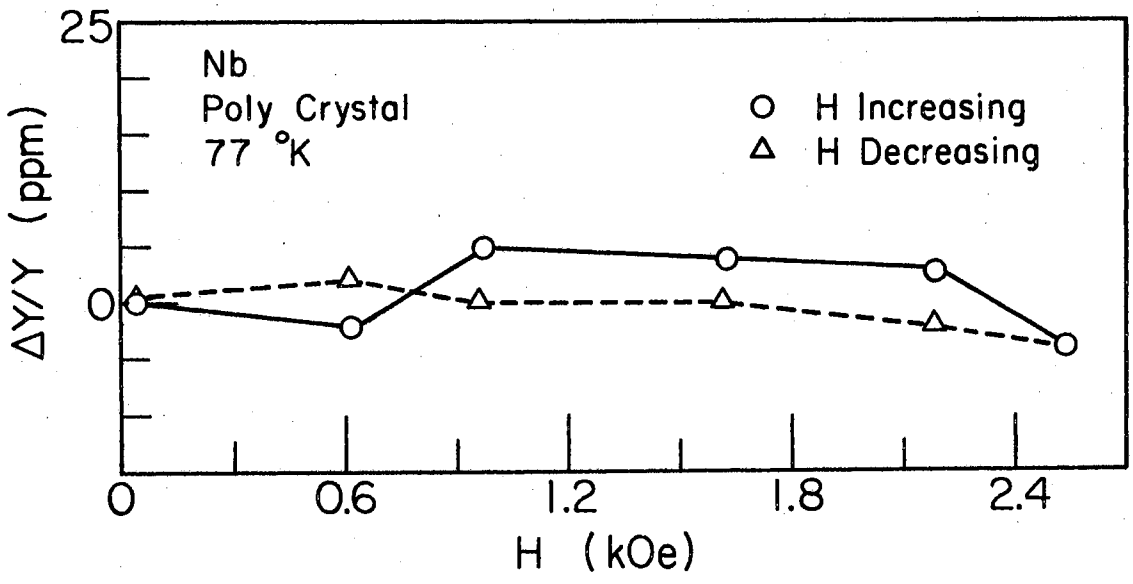

Figure 19. Poly Modulus in Normal State

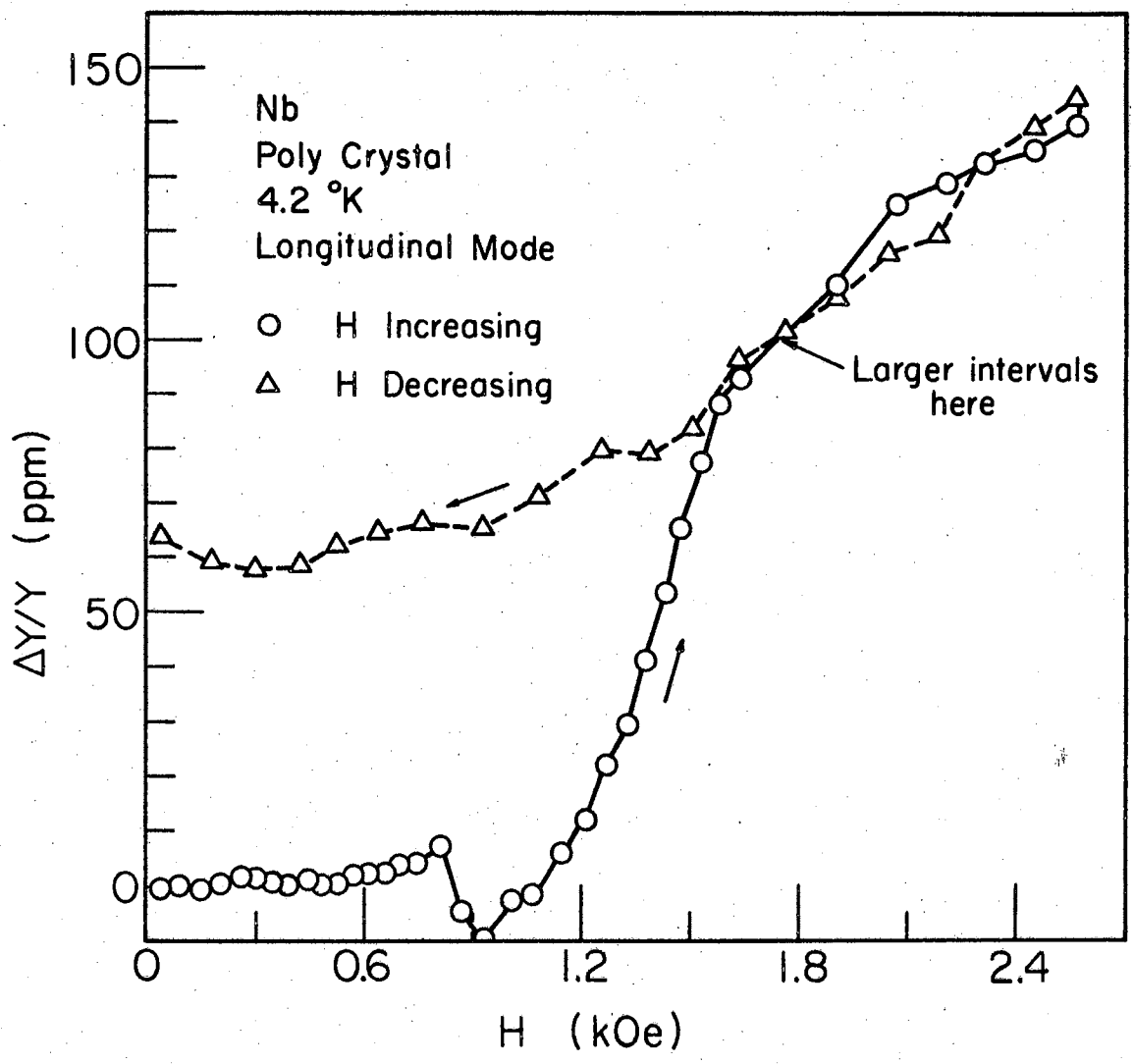

Figure 20. Poly Modulus

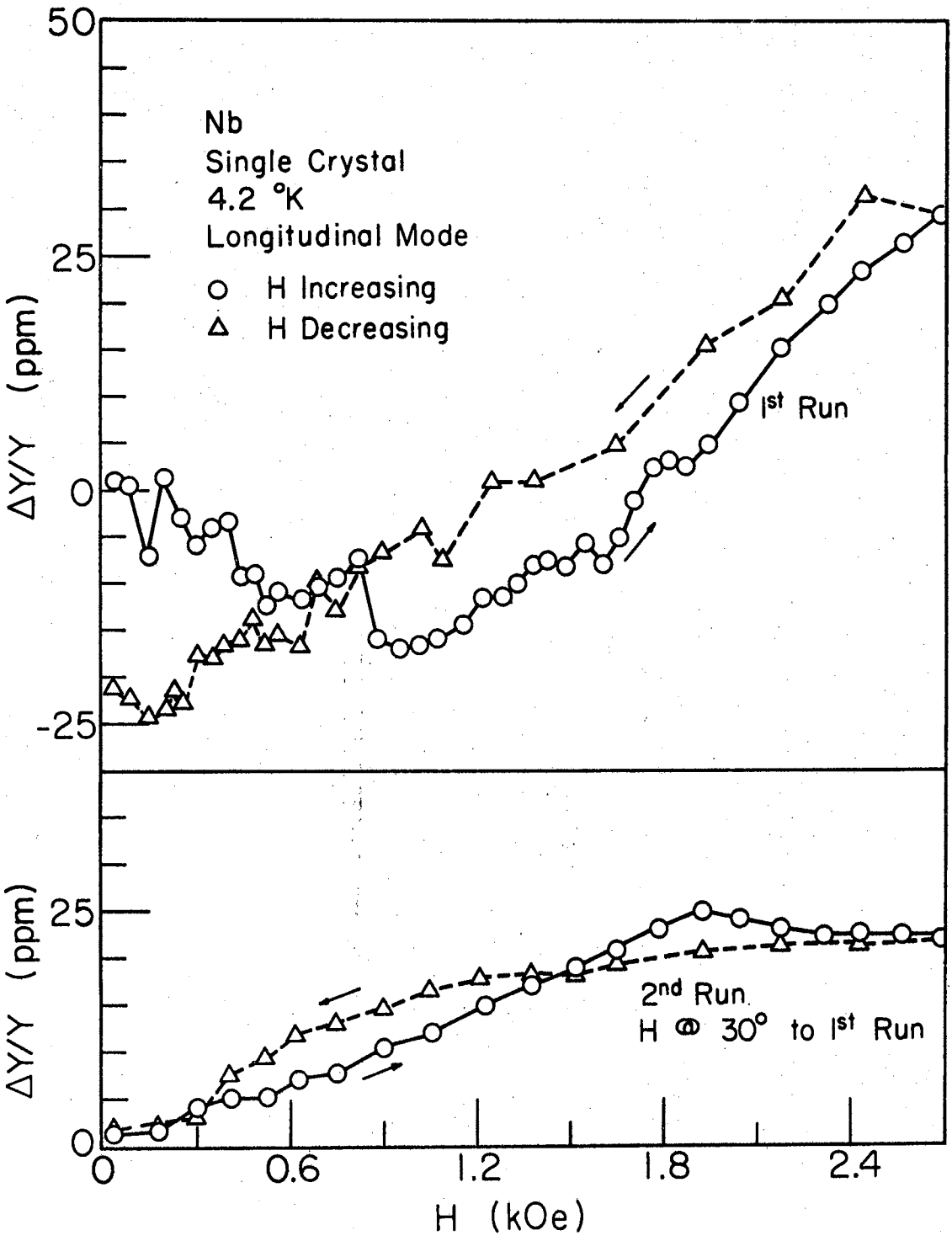

Figure 21. Single Modulus [110]

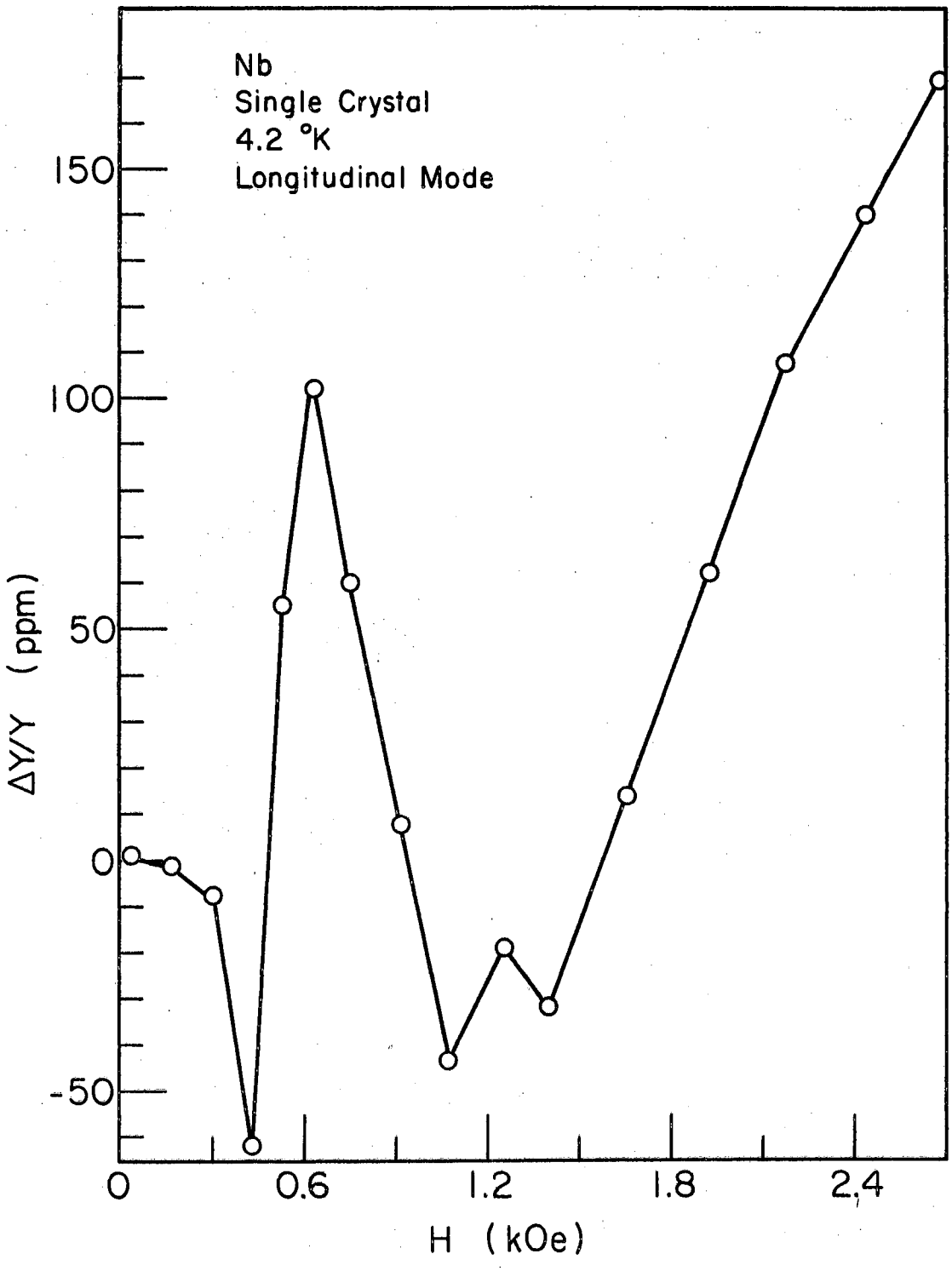

Figure 22. Single Modulus [111]

CHAPTER V

DISCUSSION

Young's modulus measurements give the most accurate results of this investigation, capable of recording changes of parts per million. Since this accuracy is attainable only in the modulus measurements, they should give the most detailed analysis of what is happening. In the temperature drift measurements, however, the drift of temperature was probably too rapid to assure sufficient thermal equilibrium for the most accurate measurements. Thus, the Bordoni peak results and the relaxation peak may only be considered as giving a rough indication of the actual shape of the curve for temperatures between 4.2°K and 77°K. The data between 50°K and 77°K can be attained more accurately by pumping on the surface of the liquid nitrogen, but this region is of little interest.

The measurements in the superconducting range depended only on the tightness of the supporting pins from run to run. The uniformity of the magnetic field was not particularly good, but at least it was a constant factor throughout the investigation. It has been shown that a more uniform field would increase H_{C1} due to a more uniform flux penetration over the surface of the material. Both the single crystal [110] and poly crystalline data indicate that H_{C1} is approximately 800 oersteds at 4.2°K. The discontinuity in Young's modulus at H_{C1} agrees with the thermodynamic arguement of a second order phase transition. A point discontinuity is apparent in the attenuation measurement. This sudden rise

and fall of the attenuation at H_{C1} could be due to a change in phase of the resonant signal with the initial flux penetration in to the specimen. The attenuation is a complex quantity in which the phase is representative of the additional impedance of the lattice to the signal velocity. Since the attenuation returns to approximately the same value after H_{C1} as it had prior to H_{C1}, this variable is also thought to be in agreement with the thermodynamics of a second order phase transition at H_{C1}.

The attenuation increases after H_{C1} as more flux enters the sample. The single crystal $[1\bar{1}0]$ data indicates flux penetrations by the ripples in the attenuation and modulus above H_{C1}. This is in agreement with the mixed state description of the region between H_{C1} and H_{C2}. However, the slope then begins to decrease prior to what is thought to be H_{C2}. Thermodynamics predicts an H_C for type II materials which is defined by the difference in Gibb's potential between the superconducting and normal states,

$$\Delta G = H_c^2/8\pi .$$

Since both the attenuation and modulus graphs show a change in slope at approximately the same field, this could be related to an H_C for type II superconductors. The change of slope near 2700 oersteds is believed to be indicative of H_{C2}. The modulus data did not reach this high field value. Thus, due to insufficient high field data, H_{C2} is not discussed further. Also, since the nitrogen temperature data showed little or no field dependence in the normal state, there was no correction taken into account for the superconducting data.

The $[11\bar{1}]$ direction data is significantly different from the other data to merit a separate discussion. Since the $[11\bar{1}]$ direction is approximately 45° off the $[1\bar{1}0]$ direction, the magnetic field is not perpendicular to the wave propagation direction. This idea coupled with the

belief that the [111] wave is partly a shear wave is sufficient argument to explain the difference between the [111] and [110] data. The difference in the data has not been reproducible due to the orientation problem of the [111] direction in the magnetic field.

On the last run magnetization measurements were taken by Gordon Nelson, Jr.[1], of this same laboratory. His measurements indicated little or no field dependence for the [111] direction and showed large changes with field in the [110] direction. This is also evidence in support of the [111] propagation as being partly shear in nature.

Agreement has also been shown with the reports of Fujii and Suzuki (9) that H_{C1} was a second order phase transition. Their work was conducted at a much higher frequency, 70 MHz, and utilizes the ultrasonic pulse technique. Since the resonant frequency method is more accurate than the ultrasonic method, it is believed to show more details.

There are many experiments that could now be conducted with the apparatus. The mixed state can be studied for various fixed temperatures below 4.2°K by reducing the vapor pressure of the liquid helium to the desired level. Flux jumps could possibly be defined from these measurements by varying the field as a function of time and recording the changes in the variables studied herein. The possibility of studying optical excitation in the mixed state by means of a laser beam would be an interesting study. Other type II superconductors, such as vanadium, tantalum, and many alloys, can be studied by this set-up, and the results could possibly lead to a satisfactory explanation of type II superconductivity.

---

[1] The use of the results of Mr. Nelson's magnetization measurements prior to publication is appreciated.

BIBLIOGRAPHY

(1) Van Buren, H. G. Imperfections in Crystals, 2nd ed. Amsterdam: North-Holland, 1961.

(2) Meissner, W., and R. Ochsenfed. "Kurze Originalmitteilungen." Die Naturwissenschaften, Vol. 21 (1933), 787-788.

(3) Kittel, Charles. Introduction to Solid State Physics, 3rd ed. New York: John Wiley and Sons, 1966.

(4) Newhouse, Vernon L. Applied Superconductivity. New York: John Wiley and Sons, 1964.

(5) Bardeen, J., N. Cooper, and J. R. Schrieffer. "Theory of Superconductivity." Physical Review, Vol. 108 (1957), 1175.

(6) Tinkham, M. "Superconductivity." Low Temperature Physics. Ed. De Witt et al. New York: Gordon and Breach, 1962, pp. 149-230.

(7) Claiborne, Lewis T., and Norman G. Einspruch. "Ultrasonic Observation of Magnetization and Flux Jumping in a Superconducting Nb-Zr Alloy." Journal of Applied Physics, Vol. 37 (1966), 925-927.

(8) Callen, H. B. Thermodynamics. New York: John Wiley and Sons, 1963.

(9) Fujii, A. I. M., and T. Suzuki. "Ultrasonic Attenuation and Magnetic Properties of Superconducting Niobium in the Mixed State." Technical Report of ISSP, Ser. A (1965), 161.

(10) Alers, G. A. "The Measurement of Very Small Sound Velocity Changes and Their Use in the Study of Solids." Physical Acoustics. Ed. Mason. New York: Academic Press, 1966, Vol. IVA, Ch. 7.

(11) Alers, G. A., and D. L. Waldorf. "Variation of the Elastic Moduli at the Superconducting Transition." IBM Journal of Research and Development, Vol. 6 (1962), 89-93.

(12) Bordoni, P. G. "Elastic and Anelastic Behavior of Some Metals at Very Low Temperatures." Journal of the Acoustical Society of America, Vol. 26 (1954), 495.

(13) Kramer, E. J., and C. L. Bauer. "Internal-Friction and Young's Modulus Variations in the Superconducting, Mixed, and Normal States of Niobium." Physical Review, Vol. 163 (1967), 407-419.

(14) Alers, G. A., and P. A. Fleury, " Modification of the Velocity of Sound in Metals by Magnetic Fields." Physical Review, Vol. 129 (1963), 2425-2429.

(15) Guess, J. F., and G. B. Thurston. "Measurement of the Flexual Response of Beams and Plates." (unpup. Research Contract Report, Oklahoma State University, 1963).

(16) Anderson, O. L. "Determination and Some Uses of Isotropic Elastic Constants of Polycrystalline Aggregates Using Single-Crystal Data." Physical Acoustics. Ed. Mason. New York: Academic Press, 1966, Vol. IIIB, Ch. 2.

(17) Niblett, D. H. "Bordoni Peak in Face Centered Cubic Metals." Physical Acoustics. Ed. Mason. New York: Academic Press, 1966, Vol. IIIA, Ch. 3.

(18) Neuringer, L. J., and Y. Shapira. "Nb-25% Zr in Strong Magnetic Fields: Magnetic, Resistive, Ultrasonic, and Thermal Behavior." Physical Review, Vol. 148 (1966), 231-246.

APPENDIX A

THERMOCOUPLE CALIBRATION PROGRAM

The program is written in Fortran IV and is given in table II. It is built to average any four emfs for one temperature and use this average emf as the mean emf for that temperature. When the average emfs are found for the three fixed points, α, β, and γ are computed. Note that one of the fixed points may not be the reference junction temperature. The computed emfs and α, β, and γ are printed, followed by a table ranging from 0.5°K to 300°K in 0.5°K steps. The table gives the delta of emf per 0.1°K, the emf, the temperature, and 1000/T.

It should be noted that this thermocouple is accurate to changes of 0.1°K. A more accurate thermocouple is the resonant frequency itself. At 77°K the frequency changes 4Hz/°K. Since changes of 0.01Hz are recorded, temperature changes of 1×10^{-4}°K can be detected. The resonant frequency changes slightly from run to run and causes calibration to be necessary for each run. However, relative changes can be observed without knowing the absolute temperature. The frequency thermocouple is useful only when other factors are known not to influence the frequency.

TABLE II

THERMOCOUPLE PROGRAM

```
$JOB   WATFOR  G.W.GOODRICH                          2233-40015
C      G W GOODRICH     THERMOCOUPLE CALIBRATION        5-24-67
       READ(5,67) TI,TO,TN,EI1,EI2,EI3,EI4
   67  FORMAT(7F10.0)
       READ(5,68) EO1,EO2,EO3,EO4,EN1,EN2,EN3,EN4
   68  FORMAT(8F10.0)
       EI =(EI1 + EI2 + EI3 + EI4)/4.0
       EO =(EO1 + EO2 + EO3 + EO4)/4.0
       EN =(EN1 + EN2 + EN3 + EN4)/4.0
       CD = TI*(TO**2*TN**3 - TN**2*TO**3) - TO*(TI**2*TN**3 - TN**2*TI**
      13) + TN*(TI**2*TO**3 - TO**2*TI**3)
       A = (EI*(TO**2*TN**3 - TN**2*TO**3) - EO*(TI**2*TN**3 - TN**2*TI**
      13) + EN*(TI**2*TO**3 - TO**2*TI**3))/CD
       B = (-EI*(TO*TN**3 - TN*TO**3) + EO*(TI*TN**3 - TI**3*TN) - EN*(TI
      1*TO**3 - TO*TI**3))/CD
       C = (EI*(TO*TN**2 - TN*TO**2) - EO*(TI*TN**2 - TN*TI**2) + EN*(TI*
      1TO**2 - TO*TI**2))/CD
       WRITE(6,73) EI,EO,EN,A,B,C
   73  FORMAT(1X,1P6E20.7)
       T = 0.00
       EMF = A*(T - 273.16)  +  B*(T - 273.16)**2  + C*(T - 273.16)**3
       T = 0.5
   74  N = 0
       WRITE(6,75)
   75  FORMAT(1H1,54H     DELTA/0.1K        EMF (MV)       TEMP K      1000/
      1TK,/)
   79  Y = EMF
       EMF = A*(T - 273.16)  +  B*(T - 273.16)**2  + C*(T - 273.16)**3
       Z = (Y - EMF)/5.0
       X = 10.0**3/T
       WRITE(6,81) Z, EMF, T, X
   81  FORMAT(1X,/,1X,F15.5,F15.5,F12.1,F12.2)
       L = 1
       GO TO 78
   69  Y = EMF
       EMF = A*(T - 273.16)  +  B*(T - 273.16)**2  + C*(T - 273.16)**3
       Z = (Y - EMF)/5.0
       X = 10.0**3/T
       WRITE(6,77) Z, EMF, T, X
   77  FORMAT(1X,2F15.5,F12.1,F12.2)
       L = L + 1
   78  IF(T-300.) 71,70,70
   71  T = T + 0.50
       N = N + 1
       IF(N-50) 80,74,74
   80  IF(L-10) 69,79,79
   70  WRITE(6,99)
   99  FORMAT(1H1)
       STOP
       END
$ENTRY
 -268.90   -195.80    24.2    -10.0605  -10.0605  -10.0605  -10.0605
 -8.2500   -8.2500   -8.2500   -8.2500   1.0568    1.0568    1.0568    1.0568
$IBSYS
```

APPENDIX B

YOUNG'S MODULUS: Y

Small variations in Young's modulus are shown to be related directly to the changes in the resonant frequency.

$$Y = Y_o + \Delta Y = Y_o(1+\delta)$$

where $\delta = \Delta Y/Y_o$ and is a function of the magnetic field, H. At $H = 0$, $\delta = 0$. The frequency is

$$f_o = v/2l = \sqrt{Y_o/\rho}/2l$$

and

$$f = (Y/\rho)^{1/2}/2l = (Y_o/\rho)^{1/2}(1+\delta)^{1/2}/2l .$$

For $\delta^2 \ll 1$,

$$(1+\delta)^{1/2} \approx 1 + \delta/2 .$$

Therefore,

$$f = f_o(1+\delta/2) .$$

$$\Delta f = f - f_o = f_o\,\delta/2$$

and

$$\delta = \Delta Y/Y_o .$$

Thus,

$$\Delta f/f_o = \tfrac{1}{2}\,\Delta Y/Y_o$$

or

$$\Delta Y/Y_o = 2\,\Delta f/f_o .$$

VITA

Gary Wayne Goodrich

Candidate for the Degree of

Master of Science

Thesis: ACOUSTICAL PROPERTIES IN SUPERCONDUCTING NIOBIUM

Major Field: Physics

Biographical:

Personal Data: Born in Dallas, Texas, July 15, 1944, the son of Mr. and Mrs. Hale C. Goodrich; married on August 26, 1967, to Patricia Anne Davison.

Education: Graduated from C. E. Byrd High School, Shreveport, Louisiana, in May, 1962; attended Centenary College, Shreveport, Louisiana, during the summer of 1962; received the Bachelor of Arts and Bachelor of Science degrees from the University of Texas in Austin, Texas, in 1966 with majors in physics; completed requirements for the Master of Science degree at Oklahoma State University in May, 1968, with a major in physics and as a National Science Foundation research assistant; became a member of Sigma Pi Sigma, physics honorary fraternity, while at Oklahoma State University.

Professional Experience: Seismic Technician, Western Geophysical Company of America, Summer 1964; Computer Operator, United Gas Company, Shreveport, Louisiana, Summer 1965; Summer Development Program, Texas Instruments, Incorporated, Summers 1966 and 1967; Graduate Teaching Assistant, Physics Department, Oklahoma State University, 1966-67; Research Assistant, Physics Department and National Science Foundation, Oklahoma State University, 1967-68.